

A Survey on Wi-Fi Sensing Generalizability: Taxonomy, Techniques, Datasets, and Future Research Prospects

Fei Wang^{ID}, Tingting Zhang^{ID}, Wei Xi^{ID}, Han Ding^{ID}, Ge Wang^{ID}

Di Zhang^{ID}, Yuanhao Cui^{ID}, *Senior Member, IEEE*, Fan Liu^{ID}, *Senior Member, IEEE*

Jinsong Han^{ID}, *Senior Member, IEEE*, Jie Xu^{ID}, *Fellow, IEEE*, Tony Xiao Han^{ID}, *Senior Member, IEEE*

Sensing Dataset Platform: <http://www.sdp8.org/>

arXiv:2503.08008v2 [cs.CV] 29 Jul 2025

Abstract—Wi-Fi sensing has emerged as a powerful non-intrusive technology for recognizing human activities, monitoring vital signs, and enabling context-aware applications using commercial wireless devices. However, the performance of Wi-Fi sensing often degrades when applied to new users, devices, or environments due to significant domain shifts. To address this challenge, researchers have proposed a wide range of generalization techniques aimed at enhancing the robustness and adaptability of Wi-Fi sensing systems. In this survey, we provide a comprehensive and structured review of over 200 papers published since 2015, categorizing them according to the Wi-Fi sensing pipeline: experimental setup, signal preprocessing, feature learning, and model deployment. We analyze key techniques, including signal preprocessing, domain adaptation, meta-learning, metric learning, data augmentation, cross-modal alignment, federated learning, and continual learning. Furthermore, we summarize publicly available datasets across various tasks—such as activity recognition, user identification, indoor localization, and pose estimation—and provide insights into their domain diversity. We also discuss emerging trends and future directions, including large-scale pretraining, integration with multimodal foundation models, and continual deployment. To foster community collaboration, we introduce the Sensing Dataset Platform (SDP) for sharing datasets and models. This survey aims to serve as a valuable reference and practical guide for researchers and practitioners dedicated to improving the generalizability of Wi-Fi sensing systems.

Index Terms—Wi-Fi sensing, Human sensing, Action recognition, Indoor localization, Domain adaptation, Domain generalization, Few-shot learning, Generative adversarial network, Transfer learning, Meta-learning

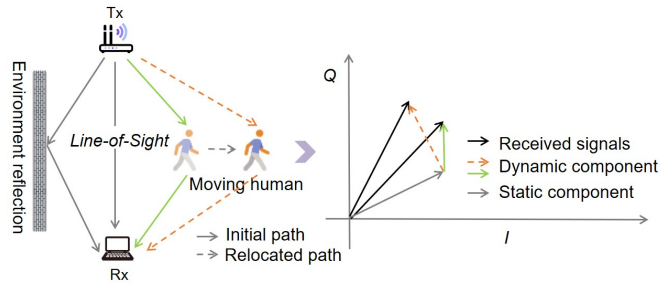


Fig. 1: Wi-Fi signals emitted from a transmitter propagate through both static environmental structures and dynamic human bodies before reaching the receiver. Human presence and movements alter the signal propagation paths, leading to measurable changes in the received signal. These variations can be leveraged for Wi-Fi sensing to interpret human movements.

Fei Wang and Tingting Zhang are with the School of Software Engineering, Xi'an Jiaotong University, Xi'an 710049, China (emails: feymanwang@xjtu.edu.cn; tt_zhang@stu.xjtu.edu.cn).

Wei Xi, Han Ding, and Ge Wang are with the School of Computer Science and Technology, Xi'an Jiaotong University, Xi'an 710049, China (emails: dinghan@xjtu.edu.cn; gewang@xjtu.edu.cn; xiwei@xjtu.edu.cn).

Di Zhang and Yuanhao Cui are with Information and Communication Engineering, Beijing University of Posts and Telecommunications, Beijing 100876, China (e-mails: amandazhang@bupt.edu.cn; cuiyuhanhao@bupt.edu.cn).

Fan Liu is with the School of Information Science and Engineering, Southeast University, Nanjing 210096, China (email: fan.liu@seu.edu.cn).

Jinsong Han is with the School of Computer Science and Technology, Zhejiang University, Hangzhou 310058, China (email: hanjinsong@zju.edu.cn).

Jie Xu is with the School of Science and Engineering (SSE), the Shenzhen Future Network of Intelligence Institute (FNii-Shenzhen), and the Guangdong Provincial Key Laboratory of Future Networks of Intelligence, The Chinese University of Hong Kong, Shenzhen, Guangdong 518172, China (e-mail: xujie@cuhk.edu.cn).

Tony Xiao Han is with the Wireless Technology Lab, Huawei Technologies Co., Ltd., Shenzhen 518129, China (e-mail: tony.hanxiao@huawei.com)

Fei Wang is the corresponding author.

I. INTRODUCTION

Wi-Fi sensing has emerged as a transformative technology that leverages ubiquitous Wi-Fi infrastructures for tasks beyond communication. By analyzing the variations in Wi-Fi signals such as Channel State Information (CSI) and Received Signal Strength Indicator (RSSI), researchers have demonstrated its potential in a wide range of applications, including activity recognition [1], [2], [3], [4], [5], [6], [7], gesture recognition [8], [9], [10], [11], [12], [13], [14], [15], [16], indoor localization [17], [18], [19], [20], [21], [22], [23], [24], user authentication and identification [25], [26], [27], [28], [29], [30], [31], health monitoring [32], [33], [34], [35], [36], [37], fallen detection [38], [39], [40], [41], [42], pose estimation [43], [44], [45], [46], [47], [48], [49], [50], crowd counting [51], [52], [53], [54], [55], and more. Many survey papers have summarized this thriving research field, reviewing existing studies from perspectives such as methods and tasks [56], [57], [58], [59], [60], [61], [62].

While Wi-Fi sensing has shown great promise across a variety of applications, its effectiveness fundamentally relies on how wireless signals interact with the surrounding environ-

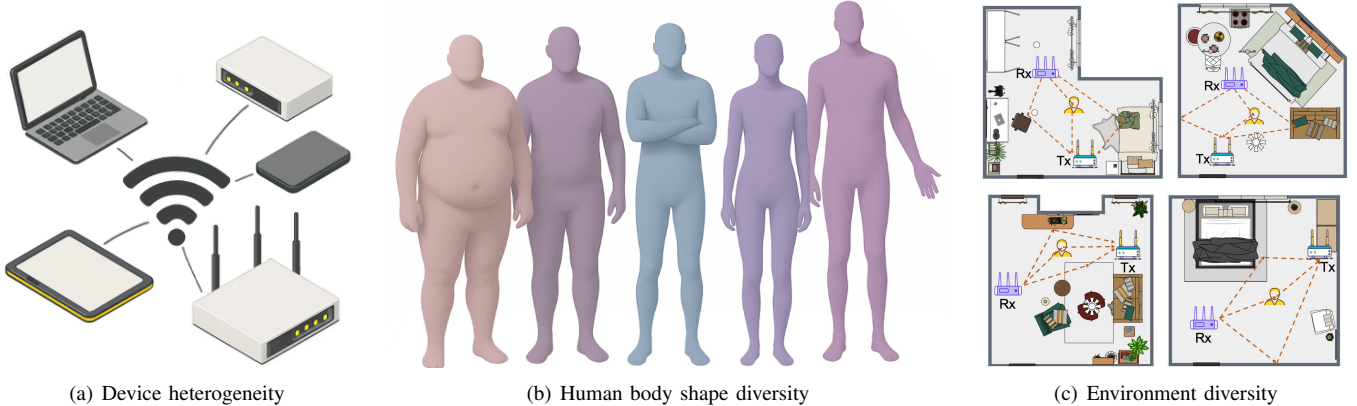


Fig. 2: Wi-Fi sensing generalization is primarily hindered by three key factors, i.e., device heterogeneity, human body diversity, and environmental diversity.

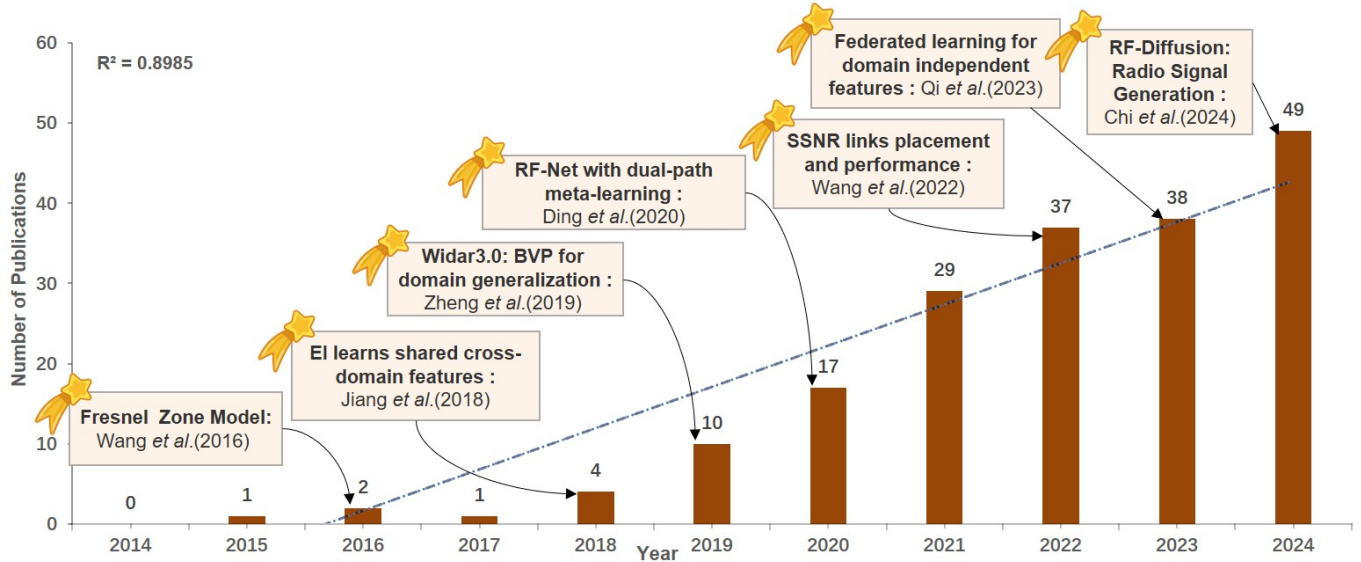


Fig. 3: Growth of research in Wi-Fi generalization: from a handful of studies between year of 2015 and 2018 to a surge of publications since 2019.

ment and the human body. Fig. 1 illustrates how human presence and motion influence the propagation of Wi-Fi signals. As shown in the figure, Wi-Fi devices are typically equipped with multiple transmit and receive antennas. Transmit antennas emit radio signals that propagate through the environment and reach the receive antennas via different paths, including line-of-sight, reflections from walls and furniture, and reflections from the human body. The presence and motion of a human subject alter the signal correlations on time, frequency or space, resulting in changes to key signal properties such as Received Signal Strength (RSS), Angle of Arrival (AoA), and Time of Flight (ToF). By analyzing these signal changes, it is possible to infer meaningful information about human activities. Both handcrafted feature-based methods and data-driven deep learning models have been developed to map variations in Wi-Fi signals to human presence, location, motion, respiration, and more—thus enabling a wide range of Wi-Fi sensing capabilities.

However, one critical challenge remains unresolved:

generalization—the performance of Wi-Fi sensing often degrades when applied to new users, devices, or environments due to significant domain shifts. This performance gap between research prototypes and practical systems arises from the inherent variability in Wi-Fi sensing conditions, which introduces considerable domain shifts across deployment scenarios. As illustrated in Fig. 2, generalization is primarily hindered by three key factors, including device heterogeneity, human body diversity, and environmental diversity. First, device heterogeneity introduces substantial signal variation. Wi-Fi signals originate from a wide range of devices—including routers, laptops, and mobile phones—that differ in protocol versions, operating channels, bandwidth, antenna design, physical orientation, and chipset configurations. These variations affect the measured CSI and RSS, often rendering models trained on one device ineffective on another. Second, human body diversity introduces non-negligible discrepancies in signal interactions. Variations in height, weight, body composition, and even clothing materials can alter the propagation

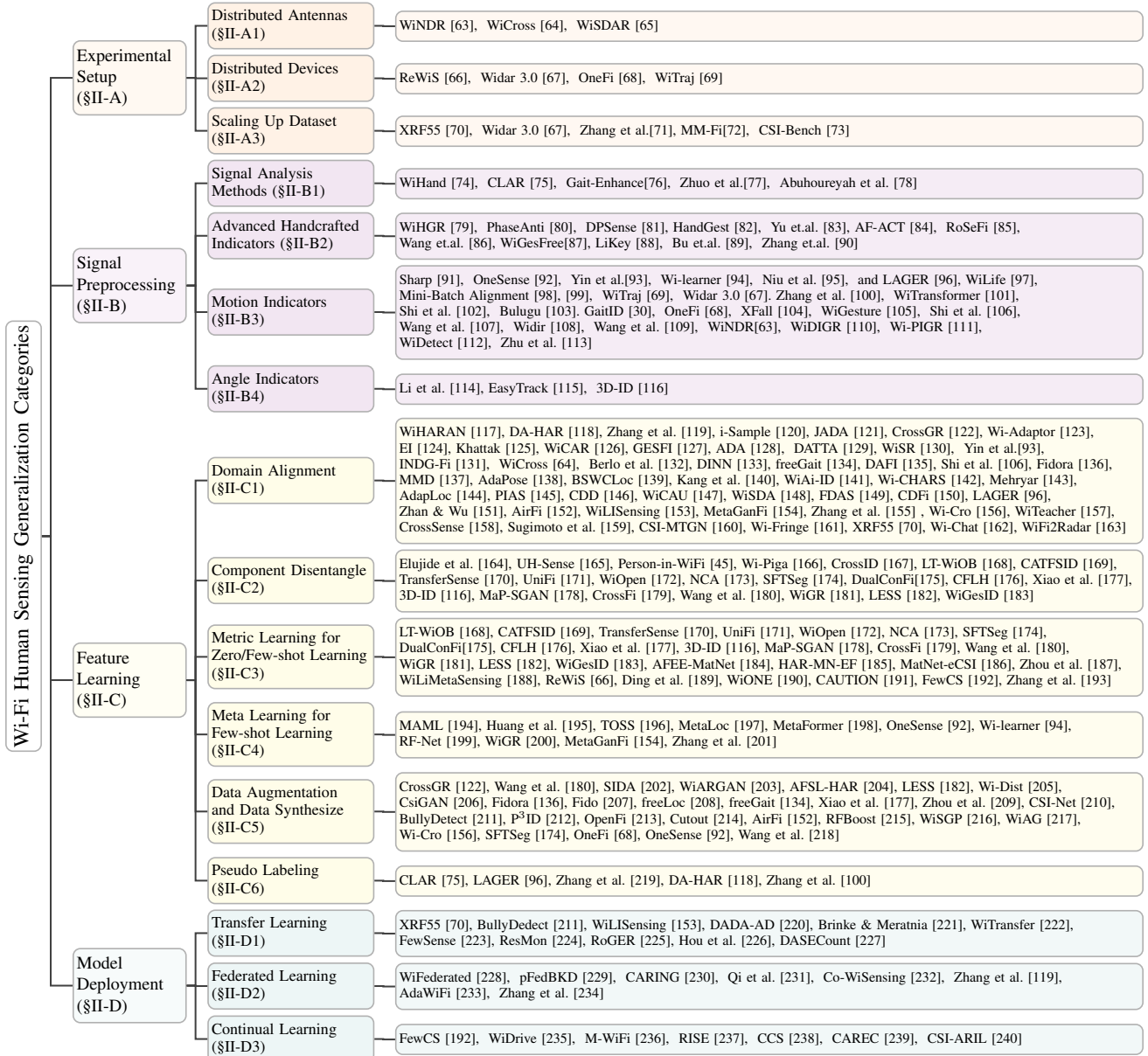


Fig. 4: We systematically review and categorize nearly a decade of research on Wi-Fi sensing generalization, covering over 200 publications since 2015. Distinct from previous surveys, we organize the literature along a four-stage sensing pipeline—device deployment, signal preprocessing, feature learning, and model deployment.

and absorption of Wi-Fi signals. As a result, two individuals performing the same action at the same location may produce significantly different signal patterns, posing challenges to consistent activity recognition. Third, environmental diversity in indoor scenes further exacerbates generalization difficulties. Differences in room layouts, wall materials, furniture placement, and device positions reshape the signal propagation paths and multipath profiles, leading to domain-specific variations in signal features such as RSS, AoA, and ToF. These changes severely limit the Wi-Fi sensing systems from generalizing beyond their training conditions.

To enhance the generalization of Wi-Fi sensing systems, a diverse array of techniques has been proposed. As shown in Fig. 3, research in this field has expanded significantly, evolving from a few studies published between 2015 and

2018 to a surge of recent work focused on improving Wi-Fi generalization. These efforts can be broadly classified into four key stages of Wi-Fi sensing systems: experimental setup, signal preprocessing, feature learning, and model deployment.

- **Experimental Setup:** The primary function is preparation and placement of devices and antennas. There are some approaches that improve generalization by strategically placing antennas around the target area or the human subject [63], [64]. This spatial diversity helps mitigate the impact of orientation changes and body blocking effects on signal reception. For instance, placing transceivers at multiple angles can reduce performance degradation caused by changes in a subject's facing direction.
- **Signal Preprocessing:** The primary function is extraction of sensing information from Wi-Fi signals, such as

denoising and signal transformation. Researchers have explored the use of domain-invariant features that are closely linked to human motion. Examples include Doppler shift and body velocity profile [67], which are more resilient to environmental variation than raw CSI or RSS data.

- **Feature Learning:** The primary function is training Wi-Fi sensing models using data. A rich set of machine learning techniques has been employed to bridge domain gaps. These include domain adaptation [241], domain generalization [242], meta-learning [194], and synthetic data generation, all aiming to learn features that are transferable across devices, subjects, and environments.
- **Model Deployment:** The primary function is deploying trained models to real-world environments. Techniques such as model fine-tuning, federated learning, and continual learning have been used to adapt pre-trained models to new settings with minimal labeled data.

This survey systematically reviews and categorizes nearly a decade of research on Wi-Fi sensing generalization, covering over 200 publications since 2015, as shown in Fig. 4. Distinct from previous surveys [243], [244], we organize the literature along a four-stage sensing pipeline—experimental setup, signal preprocessing, feature learning, and model deployment—to provide a structured and comprehensive view of existing techniques. This stage-wise organization enables researchers and practitioners to quickly identify methods suited to their specific challenges. Furthermore, we curate and summarize a wide array of publicly available datasets, offering guidance for researchers seeking appropriate benchmarks to train or evaluate generalizable models. To support future research, we also explore emerging trends, including multimodal sensing, large pre-trained models, and data-efficient learning paradigms, that are poised to shape the next generation of Wi-Fi sensing technologies. We hope this survey will serve as a comprehensive and practical resource for both newcomers and experienced researchers seeking to understand, implement, or advance generalization techniques in Wi-Fi sensing.

The remainder of this paper is organized as follows. Section II provides a stage-wise taxonomy of generalization techniques in Wi-Fi sensing, covering key methods and representative studies across device deployment, data preprocessing, feature learning, and model deployment, respectively.

Section III presents a comprehensive overview of publicly available Wi-Fi sensing datasets, categorized by sensing tasks, including action recognition, pose estimation, crowd counting, etc. Section IV discusses promising future research directions, including multimodal sensing, large-scale model pretraining, and continual learning. Finally, Section V concludes the paper by summarizing key insights on the path forward for building more generalizable Wi-Fi sensing systems.

II. TAXONOMY

To enhance the generalization of Wi-Fi sensing systems, researchers must address challenges across various stages, including device deployment, signal processing, feature learning, and model deployment. While some studies concentrate on a single stage, others tackle multiple stages simultaneously, addressing two or three phases at once. To provide a clear and systematic overview of existing research, we categorize the surveyed works based on the Wi-Fi sensing pipeline, as illustrated in Fig. 4.

A. Experimental Setup

At the experimental setup stage, some studies enhance the generalization capability of Wi-Fi sensing by adopting distributed antenna deployment, integrating additional devices, and collecting more extensive datasets, as shown in Fig. 5.

1) *Distributed Antennas:* WiNDR [63] and WiCross [64] position three antennas from the transmitter and three antennas from the receiver in a staggered, distributed manner around a 360-degree circle, with the subject performing gestures at the center. This configuration achieves direction-agnostic gesture recognition. Additionally, WiSDAR [65] tests various distributed antenna topologies, including line, hexagon, square, and random shapes, to explore regions that are most sensitive to human activities, achieving highly accurate and reliable recognition results.

2) *Distributed Devices:* Some studies utilize additional WiFi devices to enhance sensing range and improve generalization to human orientation and position. For instance, ReWiS [66], Widar 3.0 [67], and OneFi [68] adopt configurations of 1 transmitter with 6 receivers and 1 transmitter with 4 receivers, respectively, to extract environment-independent features. WiTraj [69] leverages 3 receivers placed at different viewing angles to capture human walking and

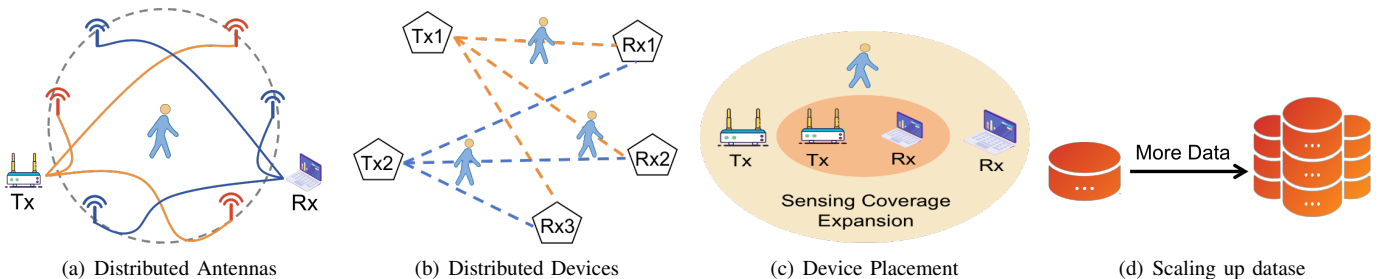


Fig. 5: In the device deployment stage, Wi-Fi generalization can be enhanced by distributing antennas to mitigate the impact of user orientation, deploying devices more widely or optimizing their placement to increase coverage, and collecting more diverse datasets to support the training of more robust and generalizable models.

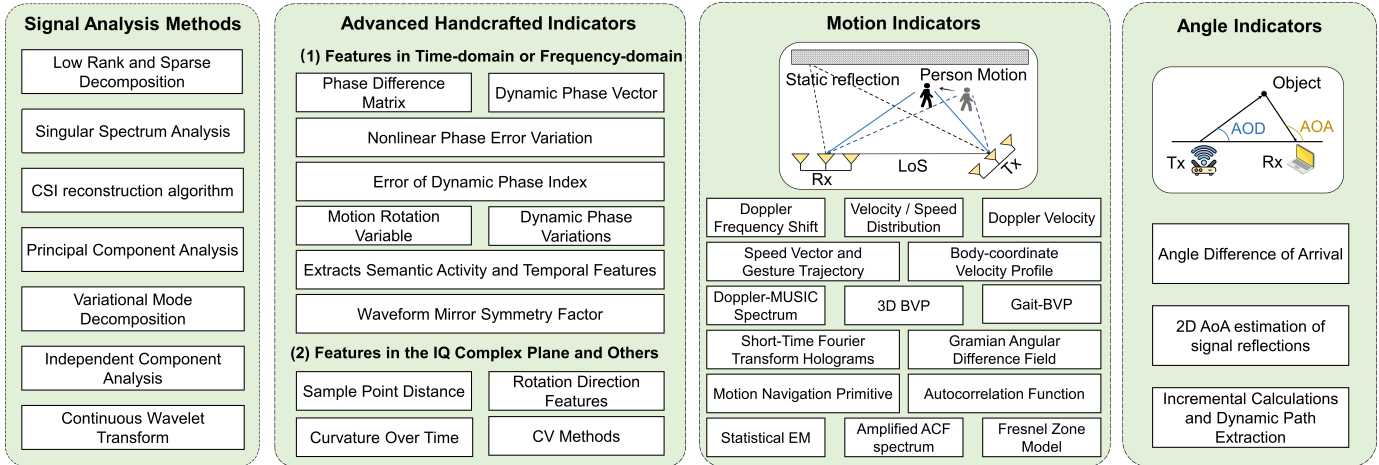


Fig. 6: Signal Preprocessing Stage

achieve robust trajectory reconstruction. Additionally, Wang et al. [245] propose a theoretical model analyzing how the distance between the transmitter and receiver influences the sensing range. Optimizing the placement of these devices effectively enhances the sensing area and reduces the impact of environmental interference.

3) *Scaling up dataset*: Scaling up training datasets is another effective approach to enhancing generalization capability, as demonstrated in Widar 3.0 [67], Zhang et al. [71], MM-Fi [72], XRF55 [70] and CSI-Bench [73]. For example, XRF55 [70] shows that training on approximately 30,000 samples enables the sensing model to naturally achieve direction and position invariance, while also supporting adaptation to new environments through few-shot fine-tuning.

B. Signal Preprocessing Stage

Many works focus on the signal preprocessing stage to extract domain-invariant features to enhance the generalizability of Wi-Fi sensing. These approaches can be broadly categorized into four types: (1) using signal analysis methods, such as Principal Component Analysis (PCA), to extract action-related features from raw signals; (2) processing phase or amplitude information to generate advanced action indicators; (3) extracting motion-specific indicators like Doppler Frequency Shift (DFS) and Body Velocity Profile (BVP) to capture dynamic movements; (4) employing antenna array techniques to derive measurements such as Angle of Arrival (AoA) and Angular Difference of Arrival (ADoA) for sensing. In the following, we introduce four categories respectively.

1) *Signal Analysis Methods*: Signal analysis plays a crucial role in Wi-Fi sensing by extracting relevant features from raw signals, ensuring generalizability across various environments, locations, and orientations. WiHand [74] employs a Low Rank and Sparse Decomposition (LRSD) algorithm to separate gesture signals from background noise, enhancing its resilience to location variations. CLAR [75] utilizes Singular Spectrum Analysis (SSA) [246] to extract the trend components from Wi-Fi signals, enabling robust activity recognition. Gait-Enhance [76] introduces a CSI reconstruction algorithm that mitigates the negative impact on recognition accuracy

caused by varying CSI patterns associated with walking in different directions. Zhuo et al. [77] apply a combination of Principal Component Analysis (PCA) and Variational Mode Decomposition (VMD) [247] to reduce noise interference in non-ideal sleep positions, enabling position-free breath detection. Abuhoureyah et al. [78] leverage Independent Component Analysis (ICA) and Continuous Wavelet Transform (CWT) to decompose CSI signals, improving multi-user human action recognition in complex environments.

2) *Advanced Handcrafted Indicators*: Many works have focused on exploring robust handcrafted features for domain-independent sensing. WiHGR [79] uses a Phase Difference Matrix to extract phase-related features. PhaseAnti [80] introduces Nonlinear Phase Error Variation (NLPEV), which is independent of Cochannel Interference (CCI), to mitigate interference and enhance recognition accuracy. DPSense [81] proposes the Error of Dynamic Phase Index (EDP-index) to evaluate the sensing quality of signal segments, prioritizing high-quality segments to improve gesture recognition performance. HandGest [82] combines Dynamic Phase Vector (DPV) and Motion Rotation Variable (MRV) for in-the-air handwriting recognition. Similarly, Yu et al. [83] extract dynamic phase features for position-independent gesture recognition. Additionally, AF-ACT [84] extracts semantic activity and temporal features to characterize activities across various locations. RoSeFi [85] identifies contextual association and waveform mirror symmetry in CSI data, introducing the Waveform Mirror Symmetry Factor (WMSF) to quantify symmetry between sit-stand postural transition (SPT) CSI data, aiding in sedentary behavior detection.

Some works also extract features in the IQ complex plane. For instance, Wang et al. [86] analyze the curvature of signal curves over time in the IQ plane. WiGesFree[87] introduces the Sample Point Distance (SPD), which uses changing CSI ratio patterns in the complex plane to capture gesture information accurately. LiKey [88] leverages rotational direction features in the CSI complex plane as an extraction of location-independent features. Other works transform Wi-Fi CSI data into images and use visual methods, such as pre-trained models and data augmentation, to improve general-

ization capabilities. Bu et al. [89] convert the amplitude of each CSI stream into a grayscale CSI image and fine-tune pre-trained networks like VGG16 and VGG19 for feature extraction. Zhang et al. [90] convert one-dimensional CSI time series into two-dimensional recurrence plots (RP) and apply data augmentation techniques like horizontal flipping, cropping, and color distortion to improve model performance and robustness in action recognition.

3) *Motion Indicators*: Many works compute domain-independent motion indicators in speed, velocity, direction, and trajectory, to enhance the generalizability of Wi-Fi sensing systems. Sharp [91], OneSense [92], Yin et al. [93], Wi-learner [94], Niu et al. [95], and LAGER [96] focus on utilizing Doppler Frequency Shift (DFS). Mini-Batch Alignment [98], [99] incorporates both DFS and Gramian Angular Difference Field (GADF). WiLife [97] further explores Doppler velocity as a key motion indicator. WiTraj [69] identifies speed ambiguity in the Doppler-MUSIC algorithm's spectrum. To address this, it employs multiple receivers at different viewing angles and leverages the CSI quotient to eliminate this ambiguity, enabling robust trajectory reconstruction.

Widar 3.0 [67] introduces the Body-coordinate Velocity Profile (BVP), which captures the power distribution across different velocities of body parts involved in gesture movements. This approach enhances generalization to new locations, environments, and subjects while maintaining performance consistency. BVP and its variants have demonstrated remarkable generalization capabilities. For instance, Zhang et al. [100] and WiTransformer [101] adopt BVP, while Shi et al. [102] and Bulugu [103] extend it to 3D BVP. GaitID [30] utilizes gait-specific BVP (gait-BVP), OneFi [68] employs velocity distribution, and XFall [104] incorporates a speed distribution profile to enhance robustness. In addition to BVP, WiGesture [105] proposes the Motion Navigation Primitive (MNP) to improve gesture recognition accuracy. Shi et al. [106] convert CSI amplitude and relative amplitude into frequency-domain representations, such as STFT holograms, to characterize the moving speeds of different body parts. Wang et al. [107] use phase changes of the reflection path to relate the speed vector and gesture trajectory in the body coordinate system, implicitly capturing the impact of position and orientation, which is estimated by a preamble gesture in each new environment.

The Fresnel Zone Model describes the signal propagation process with better interpretability, and is therefore widely used to enhance the generalization capability of Wi-Fi sensing. Widir [108] utilizes it to capture walking direction. Wang et al. [109] apply the model to detect breast motion for respiration detection. WiNDR [63] leverages the model for direction-agnostic gesture recognition. Additionally, WiDIGR [110] and Wi-PIGR [111] use the Fresnel Zone Model to eliminate direction information for gait recognition. Statistical EM methods have also been applied to Wi-Fi sensing. WiDetect [112] uses statistical EM theory to model motion detection, connecting the Autocorrelation Function (ACF) of CSI to target motion, independent of environment, location, orientation, and subjects. Zhu et al. [113] extract the Amplified ACF spectrum

from CSI, enabling motion features to be isolated, independent of environmental factors.

4) *Angle Indicators*: Angle indicators are also used to enhance the generalizability of Wi-Fi sensing. Li et al. [114] use Angle Difference of Arrival (ADoA) for location-free CSI-based activity recognition. EasyTrack [115] utilizes AoA–AoD values, leveraging changes in the length and direction of the Wi-Fi signal path. Through incremental calculations and dynamic path extraction, it can reconstruct gesture trajectories in real-time without relying on the initial gesture position or a fixed device location. 3D-ID [116] uses 2D AoA estimation of signal reflections to enable Wi-Fi to visualize a person in the environment. This visualization is then digitized into a 3D body representation using deep learning, which extracts both the static body shape and dynamic walking patterns for person re-identification.

C. Feature Learning Stage

The Feature Learning Stage is fundamental to improving the adaptability and robustness of Wi-Fi sensing systems across diverse domains. This stage includes several key techniques aimed at overcoming the challenges of domain variability, limited labeled data, and environmental changes. Methods such as domain alignment, metric learning, data augmentation, and pseudo-labeling work together to enhance model performance, ensuring that features learned from one domain can be successfully applied to others. These approaches through techniques like adversarial training, similarity metrics, data synthesis, and embedding refinement, enable Wi-Fi sensing models to generalize effectively in dynamic and heterogeneous real-world environments.

1) *Domain Alignment*: Adversarial Domain Adaptation [241], [248] aims to align the source and target domains, enabling Wi-Fi sensing to generalize across new individuals, environments, and other novel domains.

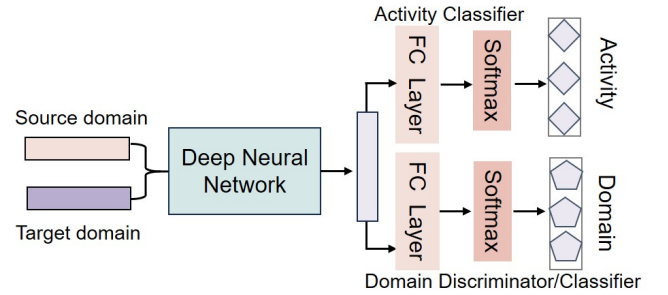


Fig. 7: Domain alignment with domain discriminator or domain classifier.

a) Domain Alignment with Domain Discriminator:

Fig. 7 illustrates a representative domain-adversarial training framework for Wi-Fi sensing generalization. The model takes both source-domain and target-domain Wi-Fi data as input and employs a deep neural network to extract shared features. These features are then fed into two branches: an action classifier for activity recognition, and a domain discriminator that attempts to determine whether the input originates from

the source or target domain. Through adversarial training, the feature extractor learns to produce domain-invariant representations that are disentangled along the domain dimension, thereby enabling more robust cross-domain activity recognition. This fundamental framework was employed in WiHARAN [117], DA-HAR [118], and Zhang et al. [119] to improve cross-environment activity recognition.

Several variants have been proposed to enhance this domain-adversarial learning framework further. For example, i-Sample [120] adopts a two-stage training strategy. In the first stage, the model focuses on learning a domain-invariant feature extractor by jointly feeding source and target domain data. A domain discriminator is used to classify the domain origin of each sample, while a parallel branch performs activity classification. In the second stage, the feature extractor is frozen, and the classifier is fine-tuned using labeled source data. This staged approach effectively enhances cross-environment generalization performance. In another line of work, JADA [121] employs two separate encoders: one for the source domain and another for the target domain. Through adversarial training with a domain discriminator, the features extracted from both encoders are encouraged to become domain-invariant. After training, the source-domain encoder is frozen, and a classification head is trained using labeled source data. The final model—comprising the target-domain encoder and the trained classification head—is used for inference on target-domain samples, achieving robust cross-domain activity recognition. Other examples are CrossGR [122] and Wi-Adaptor [123], which replace the traditional domain discriminator with an auxiliary action classifier. Unlike standard classifiers, this branch is trained to assign uniform probabilities across all action classes, effectively making actions indistinguishable in the feature space. This strategy forces the feature extractor to remove task-relevant cues from the domain-variant features, thereby encouraging it to learn more domain-invariant and task-discriminative representations. As a result, the main action classifier benefits from cleaner, more generalizable features during training.

b) Domain Alignment with Domain Classifier: Another line of work extends the domain-adversarial framework by replacing the domain discriminator with a domain classifier. While the standard domain discriminator performs binary classification to distinguish between source and target domains, the domain classifier generalizes this concept to multi-class classification, where each domain (e.g., different environments or deployment scenarios) is assigned a distinct label, also shown in Fig. 7. For example, EI [124] introduces a domain classifier to explicitly recognize the environment in which the activities are recorded. Through adversarial training, the domain classifier is optimized to correctly classify each environment, while the feature extractor is trained to fool the domain classifier, thereby learning environment-invariant representations. Similarly, Khattak and Khan [125] and WiCAR [126] adopt this strategy to achieve location-invariant activity recognition and in-car environment-invariant activity recognition, respectively.

Beyond environments and locations, user identity can also serve as a domain label. Systems such as GESFI [127], ADA [128], and DATTA [129] use the user ID as the domain

label to enable user-independent gesture recognition. This idea can be extended further: domain labels include user identity, body orientation, physical position, and environment. Building on this fine-grained decomposition, models like WiSR [130], Yin et al. [93], INDG-Fi [131], WiCross [64], and Berlo et al. [132] demonstrate the feasibility of learning representations that generalize across multiple domain factors simultaneously.

It is worth noting that this domain-classifier-based adversarial framework is not limited to activity recognition. By replacing the action classifier with other task-specific heads, this architecture has been successfully applied to a variety of tasks, including: pose estimation across subjects (e.g., DInN [133]), gait recognition across actions (e.g., freeGait [134]), indoor localization across environments (e.g., DAFI [135]), and user identification across locations (e.g., Shi et al. [106]). These extensions further underscore the versatility and effectiveness of domain-classifier-based adversarial training in improving generalization across a wide range of Wi-Fi sensing applications. In addition, Fidora [136] replaces the domain classification branch with a data reconstruction branch. In this framework, both source and target domain samples are first encoded by a shared feature extractor, and then passed through a decoder to reconstruct the original input data. The reconstruction loss serves as an indirect objective for domain alignment, encouraging the feature extractor to retain domain-invariant information that is useful for reconstruction.

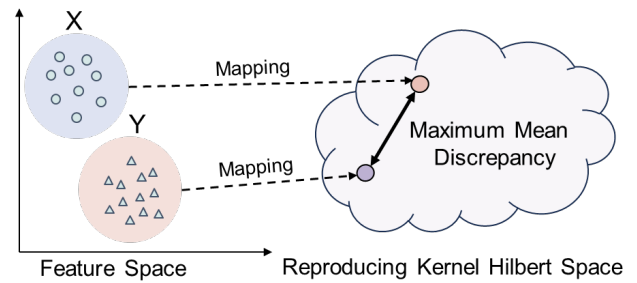


Fig. 8: Maximum Mean Discrepancy [137] quantifies the similarity between two probability distributions by projecting data into a Reproducing Kernel Hilbert Space (RKHS) and computing the squared distance between their mean embeddings, encouraging the model to learn domain-invariant representations.

c) Domain Alignment with Similarity Computing: Another widely adopted strategy for domain alignment is to explicitly minimize the distribution discrepancy between source and target domains. One representative approach is Maximum Mean Discrepancy (MMD) [137], which quantifies the difference between two probability distributions by projecting data into a Reproducing Kernel Hilbert Space (RKHS) and computing the squared distance between their mean embeddings, encouraging the model to learn domain-invariant representations, as shown in Fig. 8. In the context of Wi-Fi sensing, MMD has been successfully integrated into model objectives to mitigate domain shifts and enhance cross-domain generalization. For example, AdaPose [138] and BSWCLoc [139] utilize MMD-based alignment for cross-

environment human pose estimation and indoor localization, respectively.

Beyond standalone MMD alignment, some works combine MMD with domain classifiers to further enhance generalization. For instance, Kang et al. [140] introduce a dual-branch architecture, where MMD is applied between the source and target domains at the output of the activity classifier, while a parallel domain classifier is trained to align features across domains. This design enables robust activity recognition across variations in user identity, environment, location, and body orientation. Similarly, WiAi-ID [141] adopts MMD to align source and target features, while employing a domain classifier to discriminate appearance characteristics, achieving appearance-independent passive person identification.

In addition to MMD, several alternative metrics have been adopted to quantify distributional similarity between source and target domains. For example, Wi-CHARS [142] applies Earth Mover's Distance (EMD) to align features for cross-environment activity recognition. Mehryar [143] utilizes the Kullback–Leibler (KL) divergence to reduce domain shift, while AdapLoc [144] employs Euclidean distance for indoor localization across domains. PIAS [145] further explores Contrastive Domain Discrepancy (CDD) [146] to align representations in a contrastive manner. WiCAU [147] uses Wasserstein distance to measure to quantify distributional similarity between source and target domains.

In some cases, in addition to knowing the domain labels (e.g., environment), the class labels (e.g., action types) of both source and target domain samples are also available during training. This enables a finer-grained alignment approach, where domain-level similarity measures can be replaced by class-level distribution alignment, allowing for more precise cross-domain representation learning. A number of studies have explored this strategy under different names and formulations. For example, local MMD [249], [212], mini-batch alignment [98], [99], Multiple Kernel MMD [179], and sub-domain alignment [250] all share the common idea of aligning corresponding action classes across domains, instead of aligning the global distributions. The similarity metrics used for sub-domain alignment vary across works. For instance, P³ID utilizes Euclidean distance to measure the closeness between class features from different environments. WiSDA [148], FDAS [149], and CDFi [150] adopt cosine similarity to measure the closeness between class-conditional features from different domains. Notably, CDFi further incorporates Jensen–Shannon (JS) divergence [251] to perform an additional global domain alignment, complementing the sub-domain matching process.

In cases where only domain-level labels (e.g., environment, location) are available, but class labels of the target domain samples are unknown, some approaches generate pseudo-labels for target domain data during training to enable the above fine-grained domain alignment. For example, LAGER [96] and Zhan & Wu [151] adopt this strategy by first predicting class labels for the unlabeled target domain samples. These pseudo-labeled data are then used to perform sub-domain alignment. Both methods use Euclidean distance to measure the similarity between class-conditional feature

distributions. LAGER achieves domain generalization in cross-user, cross-person, cross-location, and cross-orientation activity recognition, while Zhan & Wu's approach targets cross-scene indoor localization.

When only multiple source domains are available during training and no target domain data is accessible, models can still improve generalization by aligning the source domains themselves. For example, AirFi [152] performs MMD-based alignment across multiple source domains, learning domain-invariant features that generalize to unseen target environments for activity recognition. Similarly, WiLISensing [153] adopts an MMD alignment strategy across source domains to train the feature extractor. During deployment, the feature extractor is frozen, and only a small number of labeled samples from the new environment are used to train the final fully-connected layers. This approach effectively enables cross-environment activity recognition with minimal adaptation effort.

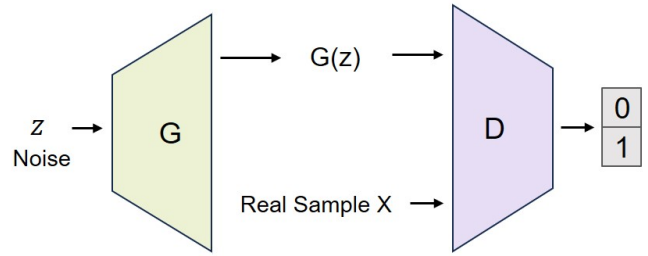


Fig. 9: Generative Adversarial Networks

d) Domain Alignment with Generative Adversarial Networks: Another line of research explores Generative Adversarial Networks (GANs) [252] to perform domain alignment by transforming data distributions or learning shared latent representations. GAN-based alignment builds on the adversarial learning mechanism of GANs, shown in Fig. 9, which involve a generator and a discriminator engaged in a minimax game. The generator aims to produce data indistinguishable from real samples, while the discriminator attempts to differentiate between real and generated data. Through iterative optimization, the generator learns to synthesize data that closely follows the expected distribution. For example, MetaGanFi [154] proposes a three-stage pipeline: (1) In the first stage, a CycleGAN-based framework [253] is used to convert Wi-Fi data from multiple source domains into a unified Uni-domain representation. This is achieved through adversarial training, where the generator transforms source-domain data to resemble a common distribution, and a discriminator is trained to identify the originating domain. The generator is optimized to fool the discriminator, thereby removing domain-specific cues. (2) In the second stage, the generated Uni-domain data are used to train an activity classifier, ensuring that the classifier learns from domain-invariant representations. (3) Finally, during inference, target-domain data are passed through the trained generator and classifier to perform activity recognition for unseen users. Similarly, Zhang et al. [155] and Wi-Cro [156] and WiTeacher [157] employ CycleGAN and StyleGAN [254], respectively, but instead of mapping source domains to a unified representation, they transform source

domain data to match the target domain distribution, thereby enabling cross-domain sign language recognition and activity recognition.

e) Domain Alignment with Multi-task Learning: Multi-task learning improves generalization by jointly training a model on multiple related tasks or domains, either through training multiple expert networks or by sharing parameters across tasks. This approach encourages the learning of representations that are both domain-invariant and task-relevant.

For example, CrossSense [158] trains 10 expert models. The experts are trained offline, and at runtime, the appropriate expert for a given input is automatically chosen. This expert selection mechanism allows the system to adaptively handle different input conditions, improving robustness across domains. Similarly, Sugimoto et al. [159] propose a system that employs a multi-task learning approach based on an encoder-decoder network architecture, where each decoder corresponds to a specific target environment. This structure ensures that the encoder learns a more general representation that can accommodate the diversity between different environments. CSI-MTGN [160] also adopts multi-task learning to learn shared parameters for the target task. Instead of using separate decoders or experts, CSI-MTGN builds a unified model where parameters are shared across multiple tasks. This shared representation facilitates knowledge transfer between tasks and domains, enhancing the model's ability to generalize from limited data. By integrating shared learning modules and task-specific heads, CSI-MTGN effectively balances generalization and specialization, making it well-suited for location-aware sensing tasks with high domain variability.

f) Domain Alignment with Cross-modal Embedding: Cross-modal alignment leverages the rich semantic information inherent in modalities such as text, images, and radar signals, which are often better understood by large-scale pre-trained models (e.g., language models or vision-language models) than raw Wi-Fi CSI. By mapping Wi-Fi data into these semantically meaningful spaces, models can benefit from external knowledge and enhanced generalization. Consequently, several works explore cross-modal embedding techniques to bridge CSI with modalities such as text, vision, and mmWave radar, enabling more robust domain adaptation.

Wi-Fringe [161] converts action class labels into BERT embeddings [255] and uses them as targets to guide the learning of Wi-Fi representations. This enables the system to bridge the semantic gap between textual activity descriptions and Wi-Fi signal patterns. Such alignment with language models facilitates better generalization to unseen activities, particularly in open-set scenarios where the label space at test time differs from training. XRF55 [70] also employs BERT embeddings as additional supervision to enhance the semantic alignment of Wi-Fi feature learning. Wi-Chat [162] goes one step further by using natural language to describe Wi-Fi signal patterns corresponding to behaviors such as walking, falling, no-event, and breathing. These descriptions are provided to a large language model (GPT-4o), enabling it to understand and interpret Wi-Fi sensing data. This approach enables zero-shot action recognition and respiratory monitoring, demonstrating a novel integration of wireless sensing with LLMs.

In addition to text-based alignment, radar signals also offer fine-grained motion information that complements Wi-Fi data. WiFi2Radar [163] proposes a cross-modal translation framework that converts CSI spectrograms into mmWave radar Doppler spectrograms using a U-Net [256] trained with synchronized radar data. This allows the model to inherit radar's high-resolution motion sensitivity while retaining the deployment convenience of Wi-Fi infrastructure.

2) Component Disentangle: Wi-Fi signals inherently contain entangled information about the environment, human presence, and motion. Several works aim to disentangle these components to enable cross-domain generalization.

For example, Elujide et al. [164] leverage unsupervised adversarial invariance [257] to disentangle gesture-related features from location-related features in the latent space, thereby enabling gesture recognition in unseen locations. UH-Sense [165] employs a GAN-based framework to denoise the data affected by UAV jitter. By filtering out motion-induced distortions, the model achieves robust human localization based on Wi-Fi signals collected from UAV platforms. Person-in-WiFi [45] assumes that Wi-Fi signals are composed of both environment-related and motion-related components. It uses a GAN to transform the signal representation into an environment-invariant latent space—one in which a domain discriminator cannot predict the environment index—thereby improving generalization for cross-environment human pose estimation. Wi-Piga [166] assumes that Wi-Fi signals contain identity-related and action-related components. It utilizes a GAN to generate features in which the identity information is no longer distinguishable. These identity-invariant features are then used for yoga pose recognition, enabling cross-user generalization. CrossID [167] leverages conditional instance normalization [258] to learn affine parameters that capture identity attributes. During inference, these parameters can be adapted to new users, enabling gesture recognition for previously unseen individuals.

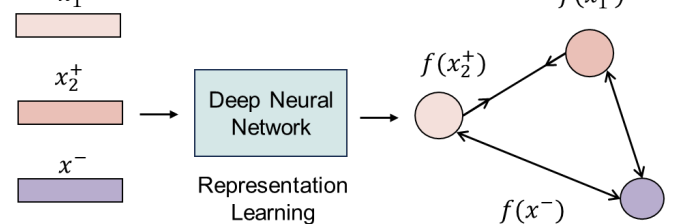


Fig. 10: Triplet loss aims to structure the feature space such that samples from the same class are mapped close together (x_1^+, x_2^+), while samples from different classes are pushed farther apart (x^+, x^-).

3) Metric Learning for Zero/Few-shot Learning: Metric learning is another important strategy for Wi-Fi sensing generalization, which aims to structure the feature space such that samples from the same class are mapped close together

(x_1^+, x_2^+) , while samples from different classes are pushed farther apart (x^+, x^-) . This is typically achieved during training by optimizing pairwise or triplet losses over sample embeddings, as shown in Fig. 10. After training, the resulting feature space forms well-separated clusters corresponding to different semantic classes.

At inference time, unlike traditional classification approaches that directly predict class labels, metric learning relies on a support set, which contains representative examples (templates) for each class. For example, in cross-environment activity recognition, the support set may consist of one labeled sample per activity from the target environment. To classify a query sample, its feature is extracted via the trained feature encoder and compared against the features of all support set samples using a similarity metric such as cosine or Euclidean distance. The class label of the closest support sample is then assigned to the query. This enables few-shot inference in the target domain with only a handful of labeled examples. Furthermore, if the support set is constructed using only training data without any target-domain samples, the model can perform zero-shot inference, which makes it particularly suitable for domain generalization scenarios.

a) Metric Learning with Triplet Loss: Several works have leveraged triplet loss, as illustrated in Fig. 10, for cross-domain few-shot Wi-Fi sensing. For example, LT-WiOB [168] and CATFSID [169] adopt the classic triplet loss strategy to train feature extractors that pull embeddings of intra-class samples closer while pushing those of inter-class samples further apart. During inference, a support set is constructed using a few labeled samples per class from the target domain. The test sample is then classified by computing distances to the support set embeddings and assigning the label of the nearest neighbor, thereby enabling cross-environment activity recognition and user identification. Similarly, TransferSense [170] employs triplet loss for cross-domain gait recognition, where the support set consists of a few samples from previously unseen users in a new environment, enabling few-shot identification based on walking patterns.

While most approaches use the standard Euclidean distance to compare embeddings, recent methods explore alternative similarity measures to improve robustness. UniFi [171] introduces a mutual information-based loss [259] to enhance discrimination between positive and negative pairs, facilitating cross-scene, cross-location, and cross-orientation activity recognition. WiOpen [172] adopts a metric learning strategy based on neighbor component analysis (NCA) [173], which minimizes intra-class distances while maximizing inter-class separability, thereby improving few-shot classification on unseen gesture classes.

Beyond handling domain and user shifts, triplet-loss-based models have also been applied to cross-modality recognition. For instance, SFTSeg [174] trains a model on the IMU-based HandGesture dataset [260] and transfers it to the Wi-Fi-based WiFiAction dataset [261], achieving few-shot recognition across sensing modalities.

b) Learning with Contrastive Learning: Contrastive learning also relies on constructing positive and negative sample pairs, and often incorporates data augmentation to

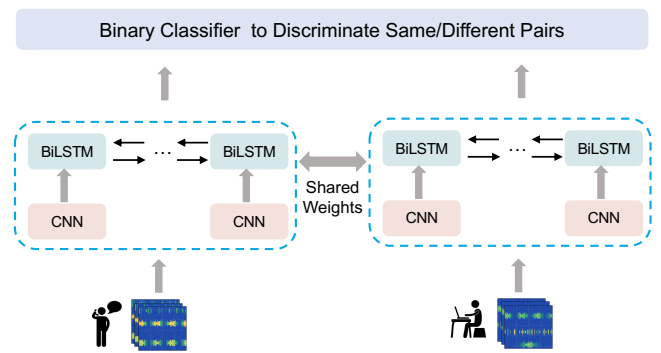


Fig. 11: Siamese Neural Networks

expand the training set. Unlike triplet loss, where each training iteration involves a single positive and negative pair, contrastive learning considers all pairwise relationships within a mini-batch. Specifically, for a mini-batch of n samples, an $n \times n$ label matrix $X = x_{i,j}$ is constructed, where each element $x_{i,j}$ indicates whether sample i and sample j belong to the same class (1) or not (0). The diagonal elements are always 1, as each sample matches itself. The loss is typically computed as a row-wise or column-wise cross-entropy over this similarity matrix, enabling the model to learn class-discriminative embeddings across all pairs in the batch. During inference, a query sample is compared with support samples in the feature space, and the label of the most similar support sample is assigned as the prediction result.

Several recent works have demonstrated the effectiveness of contrastive learning for few-shot and cross-domain Wi-Fi sensing tasks. DualConFi[175] applies a contrastive learning framework to enable robust activity recognition across different environments. CFLH [176] enhances the diversity of positive sample pairs by applying random scaling augmentations to Wi-Fi signals, and then trains the model using contrastive loss to enable few-shot recognition of unseen activities in new environments. Xiao et al. [177] further integrate diffusion-based generative modeling (e.g., Denoising Diffusion Probabilistic Models [262]) to synthesize additional positive samples. These synthetic samples are incorporated into a contrastive training pipeline, which improves the model's ability to recognize novel activities in unseen environments using limited labeled data.

c) Metric Learning with Siamese Neural Networks: Siamese neural networks [263] offer a classical yet effective architecture for few-shot learning and domain generalization. In this framework, as shown in Fig. 11, a pair of samples is fed into two identical networks that share weights. Each network extracts feature embeddings from its input, and the resulting embeddings are concatenated and passed through a binary classifier. The classifier is trained to predict whether the two inputs belong to the same class: if they do (e.g., two samples of the same activity), the target label is 1; otherwise, it is 0. During inference, a support set is constructed from a few labeled samples per class in the target domain. To classify a query sample, it is paired with each support sample and processed by the Siamese network. The network outputs a

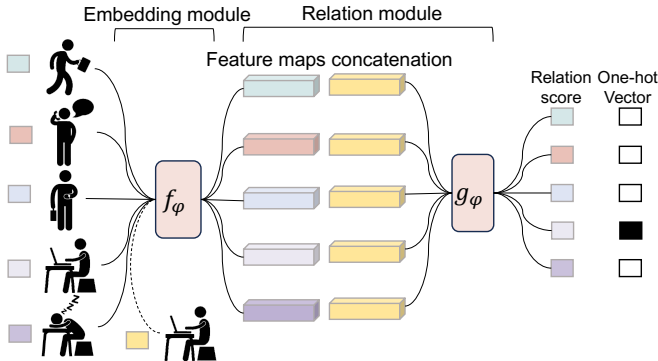


Fig. 12: Relation Network

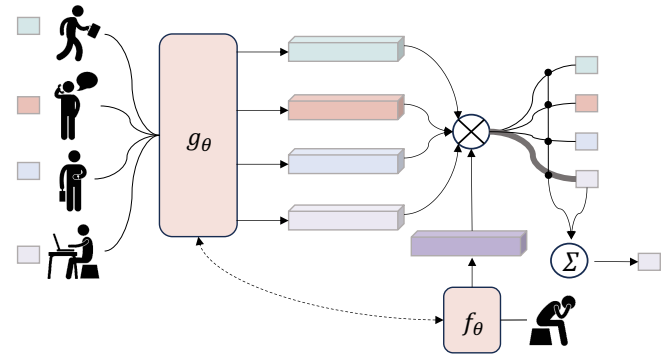


Fig. 13: Matching Network

confidence score indicating the likelihood of the two samples belonging to the same class. The class label of the support sample with the highest confidence score is then assigned to the query sample.

This pipeline has been widely adopted in Wi-Fi sensing tasks for few-shot cross-domain generalization. For instance, 3D-ID [116] utilizes this pipeline for few-shot user identification in unseen environments. MaP-SGAN [178] applies it for gait recognition by enhancing the diversity of training samples via generative models. CrossFi [179] extends the Siamese framework to handle both cross-domain and new-class scenarios, enabling gesture recognition and user identification in previously unseen domain.

d) Metric Learning with Relation Network: Relation networks [264] provide a powerful framework for few-shot learning by explicitly modeling the similarity between samples through deep relational reasoning. As illustrated in Fig. 12, training involves two components: a support set and a query set. The support set contains one labeled sample per class, while the query set contains a sample whose class is to be predicted. Both support and query samples are passed through a shared feature extractor. The resulting feature vectors are then concatenated and passed to a relation module (typically a neural network), which outputs a similarity score indicating how likely the two samples belong to the same class. The network is optimized using a multi-class cross-entropy loss, where the ground-truth label is encoded in a one-hot format: for each query sample, only the score corresponding to the matching support class is set to 1, while all others are 0. During inference, a test support set and a query sample are fed into the model. The network outputs relation scores between the query and each support sample. The class corresponding to the support sample with the highest relation score is then selected as the prediction result.

Wang et al. [180] follow the above pipeline to enable few-shot activity recognition in unseen environments. WiGR [181] adopts relation networks and trains the model on 100 action classes. To evaluate generalization to novel classes, the model is tested on previously unseen activities, using only three support samples per new class. LESS [182] also uses relation networks to achieve few-shot cross-environment fingerprint-based localization. WiGesID [183] further evaluates this framework to simultaneously support cross-environment ac-

tion recognition and user identification. Besides, WiGesID also supports few-shot classification of both new actions and unseen individuals, showcasing the flexibility of relation networks in multi-task and cross-domain scenarios.

e) Metric Learning with Matching Network: Matching networks [265] provide an effective framework for few-shot learning by leveraging attention mechanisms and episodic training to mimic test-time inference. As illustrated in Fig. 13, during training, each episode includes a support set $S = \{(x_i, y_i) | i = 1, 2, \dots, n\}$, where x_i is a sample, y_i is its corresponding label, and q is a query sample. The support set consists of a few labeled samples from each class, while the query sample is to be classified.

The predicted label of the query sample is computed as a weighted sum of the support set labels, where the weights are derived from the similarity between the query and each support sample:

$$a(q, x_i) = e^{c(f(q), g(x_i))} / \sum_{j=1}^n e^{c(f(q), g(x_j))} \quad (1)$$

$$\hat{y} = \sum_{i=1}^n a(q, x_i) y_i$$

Here, $c(f(q), g(x_i))$ computes the cosine similarity between the feature of the query sample and that of a support sample; The similarity scores are passed through a softmax function to produce the weights $a(q, x_i)$, which reflect the relative similarity between q and each x_i . The final prediction \hat{y} is obtained by weighting the support labels accordingly. As shown in the Equation. 1, samples more similar to the query contribute more significantly to the prediction.

Building on matching networks [265], AFEE-MatNet [184] and HAR-MN-EF [185] enhance domain generalization by training on data from four distinct environments and evaluating few-shot activity recognition in three unseen environments. MatNet-eCSI [186], WiLiMetaSensing [188], and Ding et al. [266] also apply matching networks to achieve cross-environment activity recognition, where each class in the support set contains one single labeled instance during inference.

f) Metric Learning with Prototypical Network: Prototypical networks [194] provide a simple yet effective approach for few-shot learning by representing each class with a prototype — the mean vector of embedded support samples. As shown

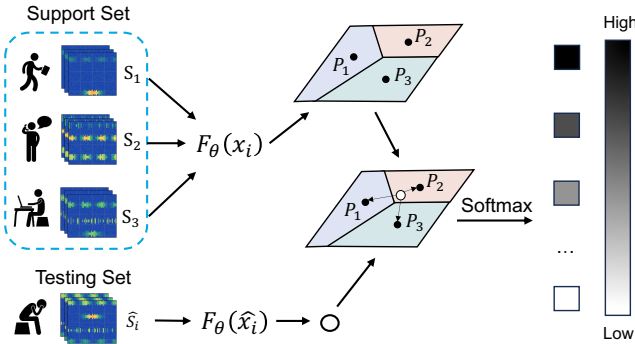


Fig. 14: Prototypical Network

in Fig. 14, training follows an episodic paradigm. In each episode, K classes are randomly sampled, with N labeled samples per class forming the support set. Each sample is passed through a shared feature encoder to extract embeddings. For each class i , its prototype c_i is computed as the mean of the support embeddings:

$$c_i = \frac{1}{N} \sum_{j=1}^N F_\theta(x_i^j) \quad (2)$$

where $F_\theta(x_i^j)$ denotes the embedding of the j -th sample from class i . To classify a query sample q , its embedding is compared to all class prototypes using a distance metric (typically Euclidean distance):

$$p(y = i|q) = e^{-d(F_\theta(q), c_i)} / \sum_{j=1}^K e^{-d(F_\theta(q), c_j)} \quad (3)$$

The resulting softmax probabilities over distances d serve as similarity scores between the query and each class prototype. The class with the highest score is the predicted label.

Several Wi-Fi sensing studies have adopted prototypical networks for few-shot cross-domain Wi-Fi sensing. For example, ReWiS [66] applies prototypical networks to compute class centroids using support samples and performs classification by measuring the Euclidean distance between the query and each class prototype, enabling cross-environment few-shot activity recognition. Similarly, Ding et al. [189] use Euclidean distance to facilitate few-shot activity recognition across different locations within the same environment. For user identification tasks, WiONE [190] computes prototype representations of each user's identity and classifies test samples based on the squared Euclidean distance to these prototypes, enabling cross-environment one-shot user authentication. CAUTION [191] adopts a similar Euclidean-distance-based framework for few-shot user authentication across scenes.

In addition to Euclidean distance, cosine similarity has also been used to compute distances between query samples and class prototypes. For instance, FewCS [192], Zhou et al. [187], and Zhang et al. [193] utilize cosine similarity to measure similarity, achieving robust few-shot activity recognition across domains such as environment, user, location, and orientation.

4) Meta Learning for Few-shot Learning: Meta learning aims to enable models to “learn how to learn”, and represents a distinct paradigm from metric learning approaches described in Section. II-C3. While both are designed for few-shot learning, metric learning focuses on constructing an embedding space where intra-class samples are pulled closer and inter-class samples are pushed apart, thereby allowing direct inference based on similarity measures. In contrast, meta learning emphasizes learning an optimal initialization or training strategy that can rapidly adapt to new tasks with only a few labeled samples. Model-Agnostic Meta-Learning (MAML) [194] is one of the most representative and widely adopted approaches.

As shown in Fig. 15, MAML employs a two-level optimization framework. In each meta-training stage, a batch of tasks is sampled from $p(\mathcal{T})$. For each task \mathcal{T}_i , the model first performs a few gradient updates using the task-specific support set, leading to adapted parameters θ_i :

$$\theta_i = \phi - \alpha \nabla_\phi \mathcal{L}_{\mathcal{T}_i}^{\text{support}}(\phi) \quad (4)$$

where ϕ is the meta-model's parameter, α is the inner-loop learning rate, and $\mathcal{L}_{\mathcal{T}_i}^{\text{support}}$ is the task-specific loss.

Then, the performance of θ_i is evaluated on the corresponding query set of each task, and the meta-objective is to optimize the model parameters ϕ so that they perform well after the inner-loop update:

$$\phi \leftarrow \phi - \beta \nabla_\phi \sum_{\mathcal{T}_i \sim p(\mathcal{T})} \mathcal{L}_{\mathcal{T}_i}^{\text{query}}(\theta_i) \quad (5)$$

where β is the meta (outer-loop) learning rate. This outer-loop update accumulates the gradients across multiple tasks, ensuring that the learned initialization ϕ is broadly effective across different domains.

During meta-testing, the model receives a new task (e.g., a new environment in Wi-Fi sensing) and is fine-tuned using just a few labeled support set samples. Thanks to the meta-learned initialization, the model can quickly converge to an effective solution with only a few gradient steps, achieving robust performance under cross-domain few-shot settings.

Huang et al. [195] and TOSS [196] employ the original MAML [194] framework to perform few-shot activity recognition across different environments. MetaLoc [197] leverages MAML for cross-scene indoor localization, demonstrating the generality of meta-learning across sensing modalities.

Beyond vanilla MAML, several studies propose MAML-like adaptations to better suit specific tasks in Wi-Fi sensing. MetaFormer [198] introduces a MAML-inspired training strategy combined with Transformer backbones, achieving one-shot cross-user and cross-environment activity recognition. OneSense [92] and Wi-learner [94] adopt similar MAML-like frameworks to handle domain shifts caused by varying environments, locations, and orientations. RF-Net [199] also applies a MAML-style strategy for one-shot activity recognition in unseen environments.

In addition, researchers have explored more recent meta-learning paradigms to improve few-shot cross-domain performance. ML-WiGR [200] incorporates Reptile [267], a

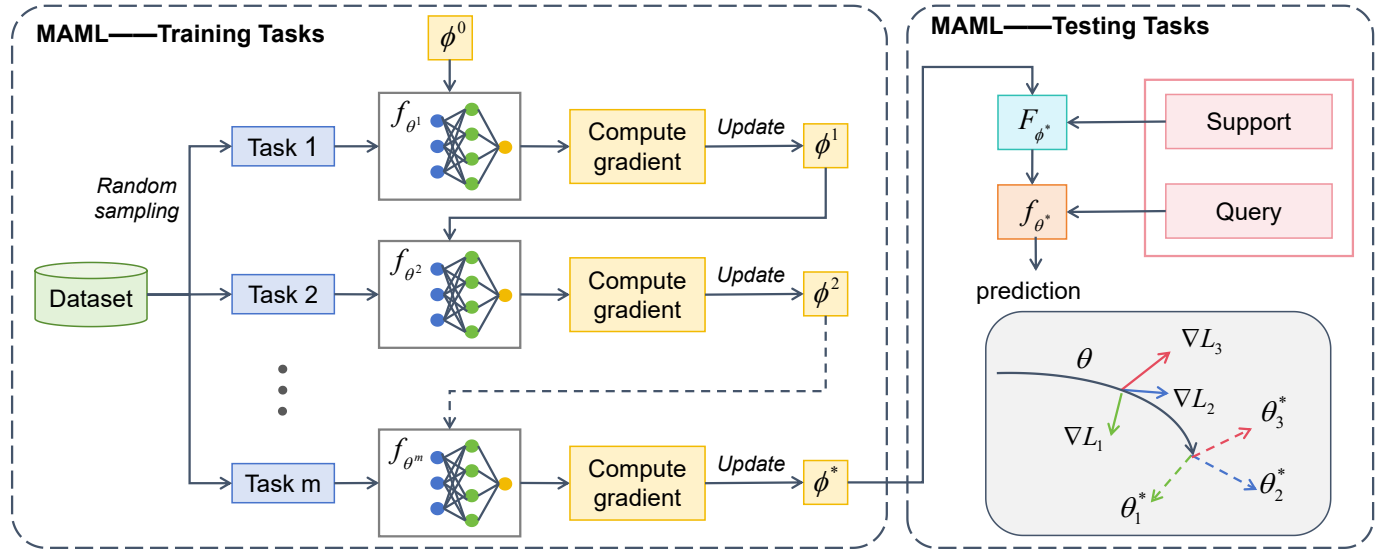


Fig. 15: Model-Agnostic Meta-Learning (MAML) [194] includes a meta-training stages and a meta-testing stage. The meta-training stage is designed to find a good initialization of model parameters such that the model can quickly adapt to new tasks with only a few gradient steps and a small amount of labeled data in the meta-testing stage.

first-order approximation to MAML, enabling efficient meta-training without second-order gradients. MetaGanFi [154] adopts the BOIL [268] method, which focuses meta-learning on the feature extractor rather than the task-specific head. Furthermore, Zhang et al. [201] utilize Learning to Learn [269], a meta-optimizer-based approach, to support cross-domain activity recognition.

5) *Data Augmentation and Data Synthesize*: Data scarcity and limited diversity are key challenges that hinder Wi-Fi sensing generalization. To address these issues, a growing number of studies leverage data augmentation and synthetic data generation. Notably, data generation is often used in conjunction with other methods, such as domain adaptation, metric learning, or meta-learning, serving as a plug-in to enhance overall sensing robustness.

Generative models like GANs, VAEs, and diffusion models are commonly employed to synthesize Wi-Fi signal data. For example: CrossGR [122], Wang et al. [180], SIDA [202], and WiARGAN [203] use GANs [252] to generate synthetic CSI data and increase data diversity. AFSL-HAR [204] and LESS [182] adopt Wasserstein GANs [270] to create more stable and realistic samples. Wi-Dist [205] and CsiGAN [206] utilize CycleGAN [253] for domain translation and data augmentation. Fidora [136] and Fido [207] employ Variational Autoencoders (VAEs) to synthesize location fingerprints. free-Loc [208] and freeGait [134] use Adversarial Autoencoders (AAEs) [271] to generate location and gait-related signals. Xiao et al. [177] apply a diffusion model [262] to produce a large number of realistic samples.

Besides generative models, various non-generative strategies are adopted to expand the training set and improve generalization: Zhou et al. [209] uses an autoencoder to synthesize action samples with one sample per action in the target domain. CSI-Net [210] augments data by combining same-class samples

to introduce intra-class variability. BullyDetect [211] applies time-series transformations such as window wrapping and window slicing to increase data volume. P³ID [212] uses magnitude warping and time permutation to augment training data. OpenFi [213] generates virtual samples with magnitude warping and Cutout [214] to train and recognize unseen actions and identities. AirFi [152] adds arbitrary Gaussian noise to create variations in the training data. RFBoost [215] proposes frequency- and time-domain augmentations to enhance signal robustness. WiSGP [216] leverages domain gradient-based augmentation to generate samples with enhanced domain diversity. WiAG [217] generates gesture variants through linear and nonlinear signal transformations.

When limited target domain data is available, augmentation strategies can be used to synthesize domain-aligned samples: Wi-Cro [156] uses CycleGAN [253] to generate synthetic samples mimicking the target domain distribution, mitigating domain shift. SFTSeg [174] employs a sliding window strategy to segment Wi-Fi signals in target domain and takes segmented signals to augment training data. OneFi [68] simulates gesture rotations to generate direction-variant samples for cross-orientation recognition. OneSense [92] generates new samples by composing gesture primitives based on signal propagation priors—e.g., combining “L” and “I” to simulate “U”—thereby enabling recognition of unseen gestures. Wang et al. [218] propose a feature decoupling approach that employs two separate classifiers to disentangle identity and gesture features. The model extracts identity-specific and gesture-specific representations independently, and then combines the gesture feature with a target user’s identity representation to generate synthetic gesture samples for that specific user for gesture recognition.

6) *Pseudo Labeling*: Pseudo-labeling, particularly the assignment of virtual labels to unlabeled target domain samples, is an effective strategy to increase training data volume,

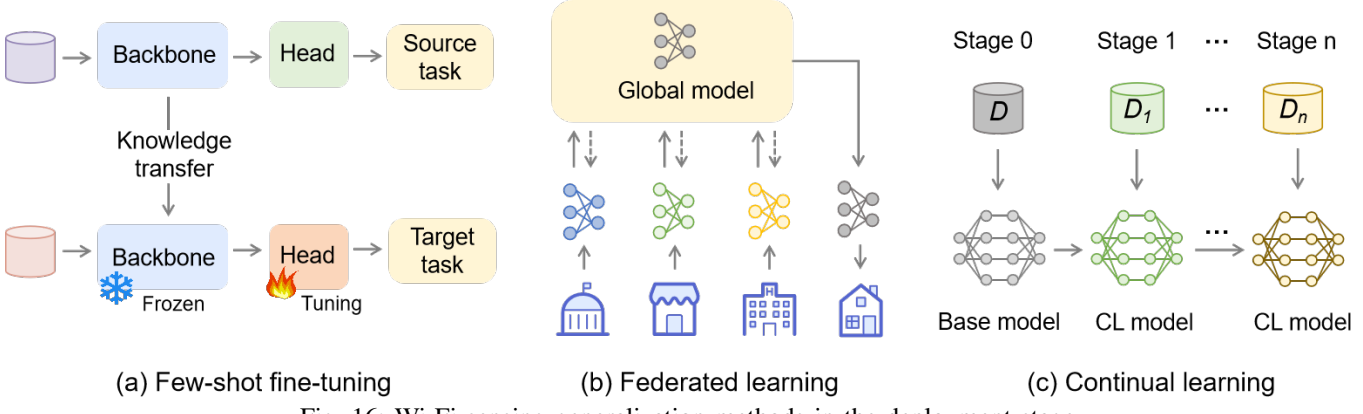


Fig. 16: Wi-Fi sensing generalization methods in the deployment stage.

enhance model generalization to unseen domains, and reduce manual annotation costs. This approach typically involves an initial feature extractor or classifier trained on source domain data, which is then used to generate labels for the target domain samples.

CLAR [75] first trains multiple classifiers on labeled source data and uses them to predict class probabilities for each target domain sample. These predictions are aggregated—typically via weighted averaging—to produce a pseudo-label. The resulting pseudo-labeled target samples are combined with labeled source data to train a unified model, thereby enabling cross-location activity recognition. LAGER [96] further refines the pseudo-labeling process by recognizing the unreliability of early pseudo-labels. It introduces a two-stage pseudo-labeling framework: after initial label assignment, the model computes the centroid of each class in the feature space, and then reassigns labels based on the distance between each target sample and the respective class centroids. This centroid-based refinement improves pseudo-label accuracy and ultimately enhances cross-domain action recognition performance.

Other works, such as Zhang et al.[219], DA-HAR[118], and Zhang et al. [100], adopt a similar strategy. They train a classifier on the source domain and use it to assign pseudo-labels to target domain samples. However, only samples with high prediction confidence (e.g., exceeding thresholds such as 0.92 or 0.8) are selected for pseudo-labeling. These high-confidence pseudo-labeled samples are then used, together with the source domain data, to retrain the classifier. The updated model generates new pseudo-labels in an iterative process, gradually improving performance on the target domain.

D. Deployment Stage

Sensing models ultimately need to be deployed, and many studies focus on enhancing cross-environment generalization during deployment or enabling models to adapt to environmental changes and meet new task requirements through continual learning after deployment.

1) *Transfer Learning with Fine-tuning*: The typical steps of transfer learning involve first training a Wi-Fi sensing model on source domain data, followed by updating the model using target domain samples, as shown in Fig. 16(a). This update can be applied to the task head, feature extractor, or the entire

model. For example, XRF55 [70], BullyDedect [211], and WiLiSensing [153] train models with source domain data and fine-tune the task head using several samples from the target domain, while freezing other parts of the model, enabling few-shot cross-domain activity recognition. DADA-AD [220] fine-tune the deep layers of the model. Besides, Brinke & Meratnia [221] experimentally compare the performance of fine-tuning the task head versus the entire network, finding that fine-tuning the whole network with 20% of target domain data yields the best results. In addition, in some cases, the target domain classification task differs from the source domain, such as in the number of action categories. To address this, WiTransfer [222] replaces the classification head and fine-tunes the new head using target domain data. FewSense [223], on the other hand, discards the classification head and fine-tunes the feature extractor using a cosine similarity loss. This loss pulls features of the same class closer while pushing features of different classes apart. During inference, it employs distance matching for classification, enabling the recognition of novel classes.

Another type of transfer learning consists of two stages: the meta-training stage and the meta-testing stage. In the meta-training stage, a rich labeled dataset from the source domain is used to train an embedding model or feature extractor. In the meta-testing stage, the embedding model is frozen, and a small number of samples from the target domain are input for feature extraction. These features are then used to fine-tune a task head, allowing the model to adapt to the target domain with limited data. Several typical works employ this framework, such as ResMon [224], which uses BayesCNN as the embedding model for domain-adaptive respiration state monitoring. RoGER [225] leverages CNN as the feature extractor to achieve domain-robust gesture recognition. Hou et al. [226] and DASECount [227] both use CNN networks as feature extractors to achieve cross-domain crowd counting.

2) *Federated Learning*: FDAS [149], WiFederated [228], pFedBKD [229], CARING [230], and Qi et al. [231] utilize federated learning frameworks to achieve efficient model deployment. As shown in Fig. 16(b), the core components include: (1) numerous clients with data collected from diverse environments, (2) a central server that trains a global model with data from diverse environments, which is expected to

possess cross-environment generalization capabilities, and (3) the distribution of the global model to client devices, where it is fine-tuned using a small amount of local data. By leveraging these federated learning principles, Wi-Fi sensing models can be effectively deployed in unseen client environments.

Some works adopt frameworks similar to federated learning but use different terminology. For instance, Co-WiSensing [232] proposes a cloud-edge collaborative framework. In this approach, a cloud server trains a cloud Wi-Fi sensing model using data from various edge devices. The higher layers of the trained model are pruned, and the lower layers are distributed to the edge devices. At the edge, the pruned model is extended with a task-specific head, which is fine-tuned using the edge user's local data to generate a Wi-Fi sensing model tailored for the edge environment. Zhang et al. [119] also employs a central server and adversarial learning to extract shared attributes across different environments. The activity-oriented attributes are then transferred to the local server, enabling cross-environment Wi-Fi human activity recognition. AdaWiFi [233] proposes a collective sensing framework, where a master device collects data using multiple sensors and trains multiple encoders collaboratively, which are then aggregated into a unified model. In the end-user environment, the model is collaboratively tuned with a small amount of labeled data. Zhang et al. [234] propose a local-global modeling method for indoor localization. The approach involves clustering Wi-Fi fingerprints of a large environment into multiple sub-areas, training local localization models for each sub-area, and then aggregating these local models into a global model. The authors demonstrate that this method achieves superior cross-environment generalization.

3) *Continual Learning*: After model deployment, it is desirable to continuously update the model to adapt to new environments or tasks, as shown in Fig. 16(c). Some works achieve this with online learning [272], a machine learning paradigm where the model learns and updates incrementally as new data becomes available. For instance, FewCS [192] collects a small amount of online data to fine-tune model parameters in new environments, enabling few-shot cross-environment human action recognition. Similarly, WiDrive [235] utilizes online model adaptation and EM algorithm [273] to update the model when in-car driver activities are misclassified, improving recognition for diverse vehicles and drivers. Unlike WiDrive's automatic error detection, the User-in-the-loop approach allows users to report misclassifications or annotate a small number of samples, which are then used to update the model. M-WiFi [236] specifically asks users to annotate critical time periods to fine-tune the trained model. To minimize the effort required from users, RISE [237] combines probability and statistical assessments with anomaly detection to identify samples that are likely to be misclassified, reducing the need for users to report every error.

Class incremental learning and domain incremental learning are also applied to enable Wi-Fi human sensing models to adapt to new activities or environments. For example, CCS [238] uses a data replay-based incremental learning approach [274], where the model is updated to sense new human activity categories using representative samples from previous

stages and samples from the current stage. CAREC [239] is a class-incremental learning framework for Wi-Fi-based indoor action recognition, effectively mitigating catastrophic forgetting [275] through dynamic model expansion and compression, and achieves high accuracy with an 80% reduction in parameters. Similarly, CSI-ARIL [240] treats the environment as a domain, updating the model with representative samples from both old and current environments. CCS, CAREC, and CSI-ARIL ensure that the model does not suffer from catastrophic forgetting when adapting to new classes or domains, preserving its ability to sense old tasks or domains.

III. DATASET

Acquiring Wi-Fi sensing data is crucial for effective Wi-Fi sensing applications. Several open-source tools are available for extracting Wi-Fi Channel State Information (CSI) and Beamforming Feedback Information (BFI), as summarized in Table I. Among these, Linux CSI Tool [276] was the earliest open-source CSI extraction tool released in 2011, while PicoScenes currently offers the most advanced CSI extraction capabilities. In addition, due to the limited availability of networks and devices supporting open CSI extraction, BFM-Tool [277] facilitates Beamforming Feedback Information (BFI) extraction, enabling Wi-Fi sensing across a broader range of devices.

TABLE I: Wi-Fi Channel State Information (CSI) and Beamforming Feedback Information (BFI) Extraction Tools

Name	max. MIMO	802.11 support	max. # subcarriers	max. bandwidth	Wi-Fi
Intel CSITool [276]	2×2	n	60	40 MHz	CSI
Atheros CSITool [18]	-	n	114	40 MHz	CSI
Nexmon CSITool [278]	4×4	n/ac	256	80 MHz	CSI
Wi-ESP [279]	2×2	b/g/n/ac	64	40 MHz	CSI
ZTE CSITool [280]	3×2	n/ac/ax	512	160 MHz	CSI
PicoScenes [281], [282]	4×4	a/g/n/ac/ax/be	1024	320 MHz	CSI
BFM-Tool [277]	4×4	ac/ax	512	160 MHz	BFI

Over the years, many researchers have generously released public datasets, significantly improving the efficiency of algorithm evaluation by removing the need to collect data from scratch. Among the various sensing tasks, activity recognition is currently the most well-represented in public datasets, as summarized in Table II. To provide a more intuitive overview of activity recognition datasets, Fig. 17 presents a bubble chart that visualizes the number of activity classes, release date, and dataset volume.

In addition, datasets are also available for tasks such as gait recognition, pose estimation, indoor localization, and temporal action localization. These datasets often include multiple domain attributes, such as environment, participant identity, and action category, making them especially suitable for evaluating generalization and cross-domain performance. In this section, we briefly introduce the domain properties of each dataset to help researchers efficiently identify the most appropriate datasets for evaluating their methods.

Furthermore, to address the scarcity of data, promote industry-academia collaboration, and foster a thriving sensing ecosystem, we have initiated and built the Sensing Dataset

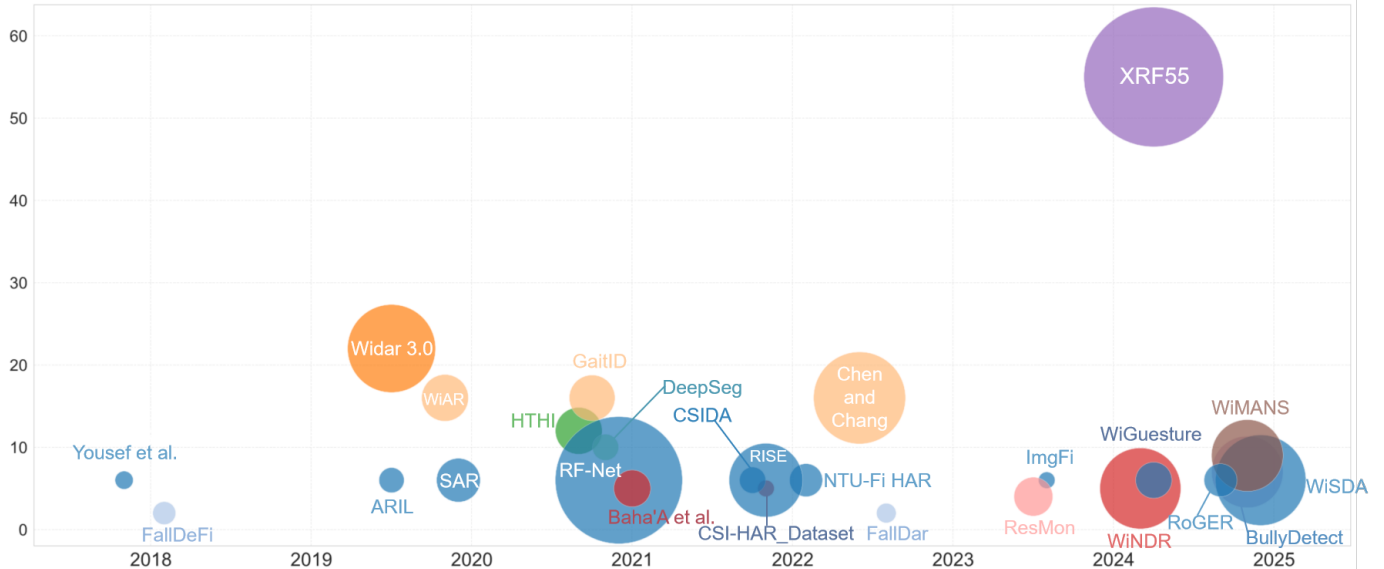


Fig. 17: Bubble chart of public Wi-Fi sensing datasets, where the bubble size indicates the number of samples and the vertical axis represents the number of classes. For visual clarity, datasets with extreme values, such as SignFi [14] (296 classes) and CSI-Bench [73] (over 1,000,000 samples), are excluded from the plot. Similarly, datasets like WiFiTAD [299], MM-Fi [72], and XRFv2 [296], which collect continuous sequences over time without clear per-sample annotations, are also not included due to the ambiguity in estimating their sample counts.

Platform (SDP, <https://www.sdp8.org/>). As the most comprehensive open repository for wireless sensing datasets to date, SDP hosts a wide range of publicly available datasets contributed by both industrial and academic communities. The platform also encourages researchers to share their own data, aiming to foster open collaboration, accelerate innovation, and support reproducible research in the field of wireless sensing.

(1) **XRF55** [70] dataset was collected in four indoor environments. In each environment, users performed 55 types of actions, categorized into five categories: human-object interactions, human-human interactions, fitness, body motions, and human-computer interactions, within a $3.1m \times 3.1m$ area. The first scene involved 30 participants, while the other three scenes involved 3 participants each. Each participant performed each action 20 times, with 42,900 samples in total, lasting 59.58 hours. The data collection setup included one transmitter with a single antenna working, and three receivers each with three antennas, arranged in a quadrilateral layout. The sampling rate was 200 Hz. Notably, XRF55 dataset also includes synchronized modalities from millimeter-wave radar, RFID, and RGB+D+IR, supporting multimodal learning and cross-modal tasks. Additionally, XRF55 also releases 2D human pose annotations for the pose estimation task.

(2) **BullyDetect** [211] dataset was collected in 8 different environments: a classroom, corridors, playgrounds, rooftops, a meeting room, a corner of the campus, an Office, and an abandoned building. Five volunteers were paired in 10 pairs, each acting as either an attacker or a victim during the experiment. The participants performed 7 different bullying actions: pushing, kicking, slapping, grabbing, punching, kneeing, and hitting with a stick. Each action was performed 5 seconds and 10 times, resulting in 11,200 samples. The experimental setup included a transmitter with a single antenna and one 3-antenna

receiver, spaced 3 meters apart, with a sampling rate of 1000 Hz.

(3) **WiSDA** [148] dataset was collected in an office setting, equipped with a desk and chair, within a $2m \times 2m$ sensing area. Three participants performed six activity categories: Push, Sweep, Clap, Slide, Draw-Z, and Draw-N. Each person collected 100 samples on 30 subcarriers and converted them to images, resulting in 3000 samples per action. The data was captured using a single pair of antennas, with one acting as the transmitter and the other as the receiver within the sensing area, similar to the setup used in the Widar 3.0 dataset. The bandwidth is 20 MHz.

(4) **WiNDR** [63] dataset was collected in an indoor office room measuring $4.8m \times 3.1m$. Three volunteers including two males and one female, aged between 25 and 30 years old and weighing between 50 to 65 kg, were asked to perform five distinct hand gestures: drawing a circle (start/accept), crossing hands (stop), clapping (switch context/menu), raising hands (increase/turn up), and lowering hands (decrease/turn down). The volunteers were instructed to perform these gestures in 24 different directions, marked by gray lines on the floor, with each direction spaced 15 degrees apart. These gestures were performed 40 times in each of the 24 directions, sampled every 15 degrees around the subjects. The collection of gesture data was facilitated by two computers, the antennas were extended with 3.5m cables and positioned 1.2m above the ground using tripods. The sampling rate was 200Hz.

(5) **WiMANS** [283] dataset was collected in three environments including a classroom, a meeting room and an empty room. Each environment was equipped with a transmitter, a receiver and a monitor camera used to capture synchronized videos. The activities were performed by five volunteers including an adult, a middle-aged person, and an elderly person.

TABLE II: Open-sourced Wi-Fi Human Sensing Datasets

ID Dataset	Main Domain Information	Device Setting	Highlight
Action Recognition			
1 XRF55 [70]	4 environments, 39 participants, 55 actions	1Tx, 3Rx, 20MHz, 5GHz	Multimodal, 55 actions
2 BullyDetect [211]	8 environments, 20 paired participants, 7 actions	1Tx, 1Rx, 20MHz, 5GHz	Bullying actions
3 WiSDA [148]	1 environments, 3 participants, 6 actions	1Tx, 1Rx, 20MHz	Widar3.0-like
4 WiNDR [63]	1 environments, 3 participants, 5 actions, 24 orientation	1Tx, 1Rx, 20MHz, 5GHz	Full 360° coverage
5 WiMANS [283]	3 environments, 6 participants, 9 actions	1Tx, 1Rx, 20MHz, 2.4/5GHz	Multi-person
6 WiGesture [284]	1 environments, 8 participants, 6 actions	1Tx, 1Rx, 100Hz, 2.4GHz	ESP32S3
7 RoGER [225]	2 environments, 4 participants, 6 actions, 4 orientation	1Tx, 2Rx, 20MHz, 2.437GHz	AR9580
8 ImgFi [285]	1 environments, 5 participants, 6 actions	1Tx, 1Rx, 20MHz	Converted to images
9 ResMon [224]	2 environments, 3 areas, 6 participants, 4 actions	1Tx, 1Rx, 20/40MHz, 2.4/5GHz	Cross-band test
10 Meneghelli et al. [286]	6 environments, 4 participants, 7 actions	1Tx, 1Rx, 80MHz, 5.21GHz	80MHz
11 Demrozi et al. [287]	2 environments, 6 participants, 6 actions	2Tx, 2Rx, 2.4GHz	Nexmon firmware
12 MM-Fi [72]	4 environments, 40 participants, 27 actions	1Tx, 1Rx, 20MHz, 5GHz	Multimodal
13 NTU-Fi HAR [288]	1 environments, 20 participants, 6 actions	1Tx, 1Rx, 40MHz, 5GHz	TP-Link N750
14 FallDar [289]	4 environments, 6 locations, 6 participants, fall & normal	1Tx, 1Rx, 1000Hz, 5GHz	6 months
15 ReWis [66]	3 environments, 2 participants, 4 actions	1Tx, 3Rx, 20/80MHz, 5GHz	80MHz
16 OPERAnet [290]	2 environments, 6 participants, 6 actions	1Tx, 2Rx, 5GHz	Multimodal
17 SHARP [91]	3 environments, 4 locations, 3 participants, 7 actions	1Tx, 1Rx, 80MB, 5GHz	80MHz
18 CSI-HAR-Dataset [291]	1 environments, 3 participants, 7 actions	1Tx, 1Rx, 20MHz, 5GHz	802.11ac
19 CSIDA [193]	2 environments, 5 locations, 5 participants, 6 actions	1Tx, 1Rx, 40MHz, 5GHz	114 subcarriers
20 RISE [237]	2 environments, 6 participants, 6 actions	1Tx, 1Rx	multi-rf devices
21 HTHI [292]	1 environment, 40 paired, 12 actions	2Tx, 3Rx, 20MHz, 2.4GHz	Human-human actions
22 DeepSeg [261]	1 environment, 5 participants, 10 actions	1Tx, 3Rx	fine-/coarse-grained actions
23 RF-Net [199]	6 environments, 11 participants, 6 actions	2 Tx-Rx pairs, 20MHz	120 environment
24 Bahaa et al. [293]	3 environments, 30 participants, 12 actions	1Tx, 3Rx, 20MHz, 2.4GHz	LOS/NLOS
25 Widar 3.0 [67]	3 environments, 5 locations, 5 orientations, 16 participants, 16 actions	1Tx, 6Rx, 20MHz, 5.825GHz	Rich domains
26 ARIL [15]	16 locations, 1 participants, 6 actions	1Tx, 1Rx, 20MHz, 2.4GHz	USRP data, clean phase
27 WiAR [294]	3 environments, 10 participants, 16 actions	1Tx, 1Rx, 20MHz, 5GHz	RSSI and CSI
28 SAR [295], [221]	1 environment, 9 participants, 6 actions	2-3Tx, 3Rx, 20MHz, 2.4GHz	6 days
29 FallDeFi [39]	5 environments, 3 participants, 9 actions	2Tx, 2Rx, 20MHz, 5.2GHz	Fall detection
30 SignFi [14]	2 environments, 5 participants, 276 gestures	3Tx, 1Rx, 20MHz, 5GHz	276 ASL Gestures
31 CrossSense [158]	3 environments, 15 locations, 100 participants, 40 actions	1Tx, 1Rx, 20MHz, 5GHz	100 participants
32 Yousef et al. [62]	1 environments, 6 participants, 6 actions	1Tx, 1Rx, 20MHz, 5GHz	Fall
Gait Recognition			
33 NTU-Fi HumanID [191]	2 environments, 20 participants, walking	1Tx, 1Rx, 40MHz, 5GHz	TP-Link N750
20 RISE [237]	3 environments, 15 participants	1Tx, 1Rx	multi-rf devices
34 GaitID [30]	2 environments, 11 participants, 8 directions	1Tx, 6Rx	8 directions
31 CrossSense [158]	3 environments, 100 participants	1Tx, 1Rx, 20MHz, 5GHz	100 participants
Pose Estimation			
35 XRFv2 [296]	3 environments, 16 participants, 30 actions	1Tx, 3Rx, 20MHz, 5GHz	Multimodal, continuous actions
36 Person-in-WiFi 3D [50]	3 environments, 7 participants, 8 actions	1Tx, 3Rx, 20MHz, 5GHz	Multi-person
1 XRF55 [70]	4 environments, 39 participants, 55 actions	1Tx, 3Rx, 20MHz, 5GHz	Multimodal, 55 actions
12 MM-Fi [72]	4 environments, 40 participants, 27 actions	20MHz, 5GHz	Multimodal
Indoor Localization			
37 MetaLoc [197]	2 environments, 180 locations	3Tx, 1Rx, 20MHz, 5GHz	RSSI and CSI
38 Chen and Chang [297]	2 environments, 16 locations	2Tx, 2Rx	CSI fingerprints
26 ARIL [15]	1 environments, 16 locations, 1 participants, 6 actions	1Tx, 1Rx, 20MHz, 2.4GHz	USRP data, clean phase
Crowd Counting			
39 SDP [298]	4 scenarios	multi-APs, 80/160MHz, 5GHz	0-2 people
40 DASECount [227]	2 environments, 2 scenarios (NLOS/LOS), 3 motions	1Tx, 1Rx, 40MHz, 2.4GHz	0-8 people
10 Meneghelli et al. [286]	1 environments, 10 participants	1Tx, 1Rx, 80MHz, 5.21GHz	1-10 people
Temporal Action Localization, Action Summarization			
35 XRFv2 [296]	3 environments, 16 participants, 30 actions	1Tx, 3Rx, 20MHz, 5GHz	Multimodal, continuous actions
41 WiFi-TAD [299]	1 environment, 3 participants, 7 actions	1Tx, 1Rx, 5GHz	Continuous actions
Multiple Sub-Datasets			
42 CSI-Bench [73]	26 environments, 35 participants	16 device configuration	In-the-wild data, 461 hours
10 Meneghelli et al. [286]	7 environments, 13 participants	1Tx, 1Rx, 80MHz, 5.21GHz	Three tasks, 80MHz
43 CSI-Net [210]	1 environments, 5 positions, 30 participants	1Tx, 1Rx, 20MHz, 5GHz	Four tasks, Biometrics

Nine activities were included in the dataset: nothing, walking, rotation, jumping, waving, lying down, picking up, sitting down and standing up. Each environment has five different locations. The dataset provides 11286 samples (over 9.4 hours) of dual-band WiFi CSI and synchronized videos.

(6) **WiGesture** [284] dataset was collected in a conference room. Eight volunteers participated in the study. The

participants performed six distinct gestures: moving left-right, forward-backward, up-down, circling clockwise, clapping, and waving. Each gesture was recorded continuously for one minute. The data collection setup consisted of a six-antenna home WiFi router acting as the transmitter and a single-antenna ESP32S3 microcontroller serving as the receiver. The transmitter and receiver were placed 1.5 meters apart, and data

was captured at a sampling rate of 100 Hz.

(7) **RoGER** [225] dataset was collected in a meeting room at two distinct locations. Location 1: A single volunteer performed six gestures, i.e., Push & Pull, Draw Zigzag, Clap, Sweep, Draw Circle, Slide, the same as Widar 3.0 [67], in four different directions. Each gesture was repeated 30 times, resulting in 480 samples. Location 2: Four volunteers (including the participant from Location 1) performed the same six gestures in four directions. Each volunteer repeated each gesture 30 times, generating 1,920 samples. Each sample lasts for 10 seconds. The setup included a two-antenna transmitter and a three-antenna receiver, operating at 2.437 GHz with a sampling rate of 100 Hz.

(8) **ImgFi** [285] dataset was collected in a laboratory, where 5 volunteers performed 6 actions: bending, drinking, nodding, squatting, drawing the letter O, and drawing the letter B. Each action was repeated 20 times. Data collection was conducted using one transmitter and one receiver positioned 4 meters apart, with the volunteers performing actions in the center. The sampling rate was 100Hz.

(9) **ResMon** [224] dataset was collected in two environments: a laboratory and a meeting room, with the laboratory further collected at two areas. Six volunteers performed 4 actions: stable breath, cough, sneeze, and yawn. The experimental setup included a two-antenna transmitter and a three-antenna receiver, operating at 2.437 GHz with a 20MHz bandwidth and sampling rate of 100 Hz. ResMon also includes samples collected at 5GHz with 40MHz bandwidth for cross-band evaluation.

(10) **Meneghelli et al.** [286] present a Wi-Fi sensing dataset collected using the 802.11ac protocol with an 80 MHz bandwidth centered at 5,210 MHz. It supports action recognition (AR), person identification (PI), and people counting (PC) tasks. For AR, four participants performed up to seven activities (e.g., walking, running, jumping, sitting still, standing still, sitting down/standing up, arm exercises) in six environments: including a bedroom, living room, kitchen, university laboratory, university office, and semi-anechoic chamber. For PI, 10 individuals were recorded moving freely in a meeting room ($7 \times 7.5 \times 3.5$ m). For PC, 1 to 10 people moved simultaneously in the meeting room. The dataset spans over 13 hours of channel state information (CSI) recordings, collected using the Nexmon tool with Netgear X4S AC2600, Asus RT-AC86U, and TP-Link AD7200 routers.

(11) **Demrozi et al.** [287] dataset was collected in two office environments. The first office, measuring $12m \times 6m \times 3m$, is divided into two blocks of workspaces, each equipped with a Raspberry Pi device and an access point (AP). The second office is smaller, $6m \times 4m \times 2.75m$, and also contains two Raspberry Pi devices and two APs. The Raspberry Pis and APs were paired to collect Channel State Information (CSI). Six participants, including two females and four males, performed five types of activities: entering the office, walking, standing, sitting, and leaving the office. The devices were arranged such that two wireless routers were placed 5 meters apart at a height of 140 cm, creating two separate 2.4 GHz WiFi networks. The total size of the dataset is approximately 70 GB.

(12) **MM-Fi** [72] dataset comprises data collected in two

rooms, 4 environmental settings, with 10 participants in each environment. The participants performed 14 daily activities, such as raising the left arm, waving the left arm, and waving the right arm, as well as 13 rehabilitation exercises, such as left front lunge and right front lunge. The setup included a transmitter with one antenna and a receiver with three antennas, arranged with a spacing of 3.75 meters between the receiver antennas. Participants performed actions while positioned 3 meters away from the receiver, facing the receiver. Each action was performed for 30 seconds. The devices operated at 5 GHz with a sampling rate of 1000 Hz. In addition to Wi-Fi sensing, MM-Fi includes data from LiDAR, mmWave radar, and camera modalities, supporting multimodal learning tasks.

(13) **NTU-Fi HAR** [288] was collected in a laboratory setting with 20 participants performing six types of actions, including running, walking, falling down, boxing, circling arms, and cleaning the floor. Each participant performed each action 20 times, resulting in a total of 2,400 samples. The setup consisted of a transmitter with one antenna and a receiver with three antennas. The equipment operated at 5 GHz with a sampling rate of 500 Hz.

(14) **FallDar** [289] dataset, developed for fall detection, was collected in two environments: a home environment and an office environment. In the home environment, five participants performed fall actions at three locations—dining room, living room, and balcony—resulting in 115 fall samples. The transmitter and receiver were placed in two settings: line-of-sight (LoS) and non-line-of-sight (NLoS). In the office environment, the transmitter was fixed in position, while the receiver was placed at 16 locations sequentially. Two participants contributed to the dataset. One performed fall actions at locations 1 and 3, while the other performed falls at locations 1 and 4. Additionally, one participant walked freely in the office to collect normal activity data. This resulted in 228 fall samples and 504 normal activity samples. In both environments, the transmitter had one antenna, and the receiver had three antennas. Data was collected at a sampling rate of 1,000 Hz with a center frequency of 5.825 GHz.

(15) **ReWiS** [66] dataset was collected in three environments: an office, a meeting room, and a classroom. Two participants performed four actions—empty room, jumping, walking, and standing—10 times in each environment, with each session lasting 180 seconds and a minimum interval of 2 hours between sessions. A Netgear R7800 Wi-Fi router with a Qualcomm Atheros chipset operated in AP mode, while an off-the-shelf laptop functioned as the client. Additionally, three Asus RT-AC86U Wi-Fi routers, each equipped with four antennas, recorded Wi-Fi CSI at a rate of 100 Hz over 20 MHz (52 subcarriers) and 80 MHz (242 subcarriers) bandwidths at 5 GHz.

(16) **OPERAnet** [290] dataset was collected in two rooms and includes data for seven activities: walk, sit, stand from a chair, lie down, stand up from the floor, rotate the upper-half body, and steady state, totaling 417 minutes of activity data. Additionally, the dataset includes 18 minutes of background data and 27 minutes of crowd-counting data. The data collection setup consisted of one transmitter with three

antennas and two receivers, each with three antennas, arranged in a right-angled triangular configuration. The second receiver was positioned at the right-angle vertex of the triangle. The sampling rate for Wi-Fi signals was 1600 Hz. OPERAnet dataset also includes synchronized data from two Kinect cameras, two UWB systems (4 nodes in system 1, 5 nodes in system 2), and a Passive WiFi Radar system constructed using a USRP-2945. This multimodal setup supports research in both multi-modal learning and cross-modal tasks.

(17) **SHARP** [91] dataset was collected in three environments: a bedroom, a living room, and a laboratory, featuring four activities—sit, walk, run, and jump—along with an empty room state. In the bedroom, volunteers P1 and P2 performed at two locations; in the living room, volunteer p1 performed at one location; and in the laboratory, volunteer P3 performed. These activities were conducted at different times over ten months. Each activity lasted 120 seconds per session, resulting in a total of 120 minutes of data. The setup included a single-antenna transmitter and receiver, along with a 4-antenna Asus RT-AC86U router as a monitoring device for collecting Wi-Fi data at a sampling rate of 173 Hz.

(18) **CSI-HAR-Dataset** [291] dataset was collected in a single indoor environment. The dataset was collected by 3 volunteers of different ages (adult, middle-aged, and elderly). Each volunteer performed seven categories of actions: walking, running, falling, lying down, sitting down, standing up, and bending. Each action was repeated 20 times by each participant, resulting in 420 samples. The experimental setup involved a Raspberry Pi 4 as the receiver and a Tp-link Archer C20 wireless router as the transmitter, operating on a 5 GHz WiFi network with a 20 MHz bandwidth on channel 36 (IEEE 802.11ac standard). The transmitter and receiver were positioned 3 meters apart, both 1 meter above the ground to ensure an unobstructed signal path. The sampling rate was 200 Hz, with 4000 samples collected over 20 seconds per activity, where the activity occurred in the middle of this period (approximately 3–6 seconds).

(19) **CSIDA**, related in WiGr [193], was collected in an office environment with three distinct locations and a classroom environment with two locations. Five volunteers performed six gestures: pull left, pull right, lift up, press down, draw a circle, and draw zigzag. Each gesture was repeated 10 times, with each repetition lasting 1.8 seconds. The device setup consisted of a single-antenna transmitter and a three-antenna receiver, separated by a distance of 2.6 meters. The system operated in the 5 GHz mode with a 40 MHz channel bandwidth, capturing 114 subcarriers with a sampling rate of 1000 Hz.

(20) **RISE** [237] dataset includes data for gesture recognition and gait recognition, collected in two environments: an office and a controlled setting with a radio frequency anechoic chamber to minimize multipath effects. Gesture Recognition: Six volunteers performed six gestures—push and pull, draw a circle, throw, slide, sweep, and draw zigzag—across ten locations (five per environment). Each gesture was repeated 30 times per location, resulting in 10,800 samples (6 volunteers \times 6 gestures \times 10 locations \times 30 repetitions). Gait Recognition: Fifteen volunteers walked under five different configurations in the controlled environment, generating 1,150 samples across

ten activity types.

(21) **HTHI** [292] dataset was collected in a furnished room. 66 volunteers participated in the study, forming 40 unique pairs to perform 12 types of human-to-human interaction activities, such as handshaking, high fives, and hugging. Each pair performed each activity 10 times, resulting in 4,800 samples. The data collection setup consisted of a commercial off-the-shelf Sagemcom 2704 router with two antennas acting as the transmitter and a desktop computer with three antennas serving as the receiver. The transmitter and receiver were positioned 4.3 meters apart. The sampling rate for the data collection was not reported.

(22) **DeepSeg** [261] dataset was collected in a meeting room with data from 5 volunteers performing 10 activities. These actions include 5 fine-grained movements such as swinging the hand, raising the hand, making a pushing motion, tracing a circular pattern (O), and tracing a cross pattern (X), as well as 5 coarse-grained activities, namely boxing, picking up an object, running, squatting down, and walking. Each participant repeated each action 30 times, resulting in 1,500 samples. The dataset collection setup included a single-antenna transmitter and a three-antenna receiver placed 2 meters apart, with a sampling rate of 50 Hz.

(23) **RF-Net** [199] dataset was collected in six different rooms with 11 volunteers performing six types of actions: wiping, walking, moving, rotating, sitting, and standing up. The Wi-Fi setup included two transmitter-receiver pairs, operating at a sampling rate of 100 Hz.

dataset was collected in six different rooms with 11 volunteers performing six types of actions: wiping, walking, moving, rotating, sitting, and standing up. The Wi-Fi setup included two transmitter-receiver pairs, operating at a bandwidth of 20 MHz and a sampling rate of 100 Hz. Each participant performed each action 20 times in 100 environments, resulting in 12,000 samples.

(24) **Baha'A et al.** [293] data collected in three different environments: two with line-of-sight (LOS) settings and one with a non-line-of-sight (NLOS) setting. Thirty volunteers performed five different actions: falling from a sitting position, falling from a standing position, walking, sitting down and standing up, and picking up a pen from the ground. Each action was performed 20 times. The experimental setup included a single-antenna transmitter and a three-antenna receiver, operating at a frequency of 2.4 GHz with a sampling rate of 320 Hz.

(25) **Widar3.0** [67] dataset was collected in three environments: a classroom, a spacious hall, and an office room. In each environment, volunteers performed actions within a $2\text{m} \times 2\text{m}$ area, with five designated locations and five orientations at each location. The dataset includes two types of hand gestures. The first type consists of general hand movements, including pushing and pulling, sweeping, clapping, sliding, drawing circles, and drawing zigzags. The second type involves drawing the numbers 0~9. The first type of action was performed by 16 participants, resulting in 12,000 samples ($16 \times 5 \times 5 \times 6 \times 5$ instances), while the second type was demonstrated by 2 participants, with 5,000 samples ($2 \times 5 \times 5 \times 10 \times 10$ instances). Widar3.0 was collected using a transmitter with one antenna

and at least three receivers, each with three antennas. The dataset was captured on channel 165 at 5.825 GHz with a sampling rate of 1,000 Hz.

(26) ARIL [15] dataset was collected in a $3.2\text{m} \times 3.2\text{m}$ area within a laboratory, with 16 positions. The actions include 6 hand gestures for potential human-computer interaction applications: hand up, hand down, hand left, hand right, hand circle, and hand cross. One volunteer performed each gesture 15 times at each position. The dataset contains a total of 1,394 valid samples. Data was collected using two USRPx210 devices, each with a single antenna, as transmitter and receiver. The sampling rate was approximately 60 Hz.

(27) WiAR [294] dataset was collected in three indoor environments: one empty room, one meeting room, and one office, as well as two outdoor environments, including a playground and a corridor. Ten volunteers performed three categories of actions: upper body activities, lower body activities, and whole-body activities, with 16 different actions. Each action was performed 30 times. The experimental setup included a transmitter with a single antenna and one receiver with three antennas, spaced 4 meters apart. The participants performed the actions at the center of the setup.

(28) SAR [295], [221] dataset was collected in the living room of an apartment. A total of 9 volunteers participated in experiments over 6 days. During the first 3 days, 3 different volunteers participated each day, while 2 volunteers participated repeatedly over the last 3 days. During the first 3 days, participants performed 6 actions: Clap, Walk, Wave, Jump, Sit, and Fall. In the last 3 days, participants performed the same actions except for Jump, resulting in a total of 5 actions. Each action was performed continuously for 5 seconds and repeated 50 times. The data collection setup consisted of a transmitter and a receiver, each equipped with three antennas, spaced approximately 2.5 meters apart. The sampling rate was 20 Hz.

(29) FallDeFi [39], designed for fall detection, was collected in five environments: a kitchen, bedroom, corridor, laboratory, and bathroom. Three participants performed fall actions and other activities such as walking, jumping, sitting down, and standing up, with each action lasting for 10 seconds and 1153 samples in total. Each environment featured one transmitter and one receiver, with varying placement distances between 4 and 9 meters depending on the setting. To introduce environmental variations, data was collected on different days, and the transmitter's position was adjusted during the experiments. All experiments were conducted at 5.2 GHz with a sampling rate of 1000 Hz and a bandwidth of 20 MHz.

(30) SignFi [14] dataset was collected in two environments: a laboratory and a home. The lab, measuring $13\text{m} \times 12\text{m}$, the distance between the AP and the STA was 230 centimeters. While the home environment, with dimensions of $4.11\text{m} \times 3.86\text{m}$, offered a shorter distance of 130 centimeters between the AP and STA. 5,520 instances were recorded in the lab, while the home environment provided 2,760 instances. The data involved 276 different sign language gestures, encompassing movements of the head, arm, hand, and fingers. The gestures were performed by 5 different users, and the users were instructed to perform each sign gesture repeatedly, with

20 instances for the lab environment and 10 instances for the home environment, resulting in a total of 8280 gesture instances. The experiments were conducted at 5 GHz with a bandwidth of 20 MHz.

(31) CrossSense [158] dataset was collected in three scenarios: a hall entrance, a narrow corridor, and a room, with the participation of 100 volunteers. For gait recognition, each volunteer walked 20 times in the same direction in each scenario, resulting in a total of 6,000 samples. For action recognition, five predefined positions were set in each scenario. At each position, each volunteer performed 40 different actions (e.g., pull, kick, throw), repeating each action 10 times. This resulted in a total of 600,000 samples. The experimental setup included one transmitter and one receiver, both equipped with three antennas. The devices operated at 5 GHz with a sampling rate of 1,000 Hz.

(32) Yousef et.al. 2017 [62] dataset was collected in an indoor office area where the WiFi transmitter and receiver were positioned 3m apart in a line-of-sight (LOS) condition. Six volunteers performed six different activities: lying down, falling down, walking, running, sitting down, and standing up. Each activity was performed 20 times, yielding 720 samples, and each activity was recorded for 20 seconds. Additionally, video recordings were made during the experiments to help label and annotate the activities in the dataset. The sampling rate was 1000 Hz.

(33) NTU-Fi HumanID [191] dataset was collected in a laboratory and a cubic office. Twenty volunteers, including 12 males and 8 females aged between 20 and 28, participated in the experiments, with 15 designated as legal users and the remaining as illegal intruders. Volunteers walked individually through the testing area, and their gait was captured using WiFi signals. Two TP-Link N750 routers were used: one as a transmitter with a single antenna, operating in 802.11n AP mode at 5 GHz with a 40 MHz bandwidth, and the other as a receiver with three antennas.

(34) GaitID [30] dataset is designed for gait recognition tasks. Data was collected in two scenarios: a hall and a discussion room. Volunteers walked along four predefined tracks, each with two walking directions (starting from both ends of each track). In the hall, 10 volunteers participated, with each walking 50 times in each direction. In the discussion room, 3 volunteers repeated each track 25 times in each direction. A total of 4,600 samples were collected. The data collection setup included one transmitter and six receivers, forming six Wi-Fi links. The sampling rate, bandwidth, and center frequency were not reported.

(35) XRFv2 [296] dataset is designed for continuous action localization and action summarization. It was collected in three distinct indoor settings—a study room, a dining room, and a bedroom. In each environment, 16 volunteers performed continuous actions spanning 30 categories. The dataset comprises 853 continuous action sequences, each lasting approximately 80 seconds, making it suitable for continuous action detection, localization, and summarization tasks. The data collection setup utilized one transmitter and three receivers with a sampling rate of 200 Hz. In addition to WiFi measurements, participants wore six IMU sensors placed on an earphone,

glasses, two phone pockets, and two wrist-worn watches. Furthermore, XRFv2 provides pose annotations, supporting multimodal fusion and cross-modal research.

(36) Person-in-WiFi 3D [50] dataset was collected in three environments: an office, a classroom, and a corridor, each within a $4\text{m} \times 3.5\text{m}$ area. Seven participants freely performed eight actions: reaching out, raising hands, bending over, stretching, sitting down, lifting legs, standing, and walking. In addition to scenarios with a single participant, there were also cases where 2, 3, or 4 participants simultaneously performed actions within the scene. Each clip was recorded for 40 seconds, resulting in a total of 456 40-second recordings. The data collection setup included one transmitter with a single antenna and three receivers, each with three antennas, arranged in a quadrilateral layout. The sampling rate was 200 Hz.

(37) MetaLoc [197] dataset was designed for indoor localization and collected in a $12\text{ m} \times 5\text{ m}$ hall and a $10\text{ m} \times 8\text{ m}$ laboratory. In each environment, Wi-Fi fingerprints (RSS and CSI) were recorded at 90 grid points. The setup included three transmitters: an ASUS RT-AC86U, a TP-Link TL-WR885N, and a TP-Link TL-WR886N, and a Nexus-5 smartphone as the receiver. The system operated at 5 GHz with a bandwidth of 20 MHz.

(38) Chen and Chang [297] released a dataset used for WiFi fingerprinting localization tasks. Data was collected in two different environments: a conference room and a cubicle office. In the conference room, data was collected at 16 locations, with 600 samples recorded at each location. In the cubicle office, data was collected at 18 locations, with 500 samples recorded at each location. The data acquisition system in the conference room consisted of one fixed-location transmitter-receiver pair, each equipped with two antennas, with a distance of 6 meters between them. In the cubicle office, the data acquisition system consisted of two fixed-location transmitter-receiver pairs, each equipped with two antennas. The number of volunteers participating in data collection, sampling rate, bandwidth, and center frequency were not reported.

(39) The SDP dataset [298] is an industrial-grade WiFi sensing dataset tailored for person detection and counting tasks, featuring realistic deployments in both home and office scenarios. In the home setting, two scenarios are included, each consisting of three rooms—one parlor equipped with an access point (AP) and two bedrooms with replay devices. Each device is equipped with two antennas and operates at 5GHz using the 802.11ax protocol, with a sampling rate of 20Hz and bandwidths of 80MHz or 160MHz. Up to two people may be present and moving in each room, and a sweeping robot is introduced as an additional source of interference. The office setting includes two scenarios: the first features four rooms, each with an AP and four-antenna devices, operating on the 5GHz band with 802.11ac and 20MHz bandwidth; the second involves a corridor with three APs placed at the left, center, and right, and four adjacent rooms without APs. This scenario captures up to two occupants per room and includes varying sampling rates—5Hz, 20Hz, 30Hz, 50Hz, and 100Hz—to explore the effect of temporal resolution.

(40) DASECount [227] dataset, designed for crowd count-

ing, was collected in two environments: an office and a lecture hall, each with both line-of-sight (LOS) and non-line-of-sight (NLOS) configurations, resulting in four different environmental settings. Volunteers, ranging from 0 to 8 people, performed three types of motion: static (seated with free actions like eating or typing), dynamic (random walking), and mixed (unrestricted activities including walking and sitting). Each sampling sequence was recorded for 5 minutes. The experimental setup included a two-antenna transmitter and a three-antenna receiver, operating at 2.4 GHz with a bandwidth of 40 MHz and a sampling rate of 100 Hz.

(41) WiFiTAD [299] is a dataset specifically designed for temporal action detection. It was collected in a single office with size of $7\text{m} \times 12\text{m} \times 2.5\text{m}$, where participants continuously performed a sequence of seven actions between the transmitter and receiver, including walking, running, jumping, waving, falling, sitting, and standing. The dataset comprises a total of 553 action sequences, each with an average duration of 85 seconds. Data were collected from 3 volunteers using a laptop equipped with an Intel 5300 NIC, configured with one transmitter and one receiver, each having a single antenna, with a sampling rate of 100Hz.

(42) CSI-Bench [73] is a comprehensive, in-the-wild WiFi sensing benchmark that integrates multiple classification-oriented sub-datasets to support a wide range of sensing tasks. These include fall detection (6 environments, 17 participants, 6,700 samples), breathing detection (3 environments, 3 users, 100,000 samples), motion source recognition (10 environments involving 13 humans, 20 pets, a robot, and a fan), room-level localization (6 environments, 8 users), user identification (6 users), activity recognition (5 activity classes), and proximity recognition (4 distance levels). A key strength of CSI-Bench lies in its emphasis on realism: data are collected using commercial WiFi edge devices across 26 diverse indoor environments with 35 real users. Spanning over 461 hours of effective recordings, CSI-Bench captures rich signal variations under natural, uncontrolled conditions, making it a valuable resource for evaluating the generalization, robustness, and scalability of WiFi sensing algorithms.

(43) CSI-Net [210] is a multi-task WiFi sensing dataset collected in a single indoor environment ($5\text{m} \times 6\text{m}$) using one transmitter and one receiver, each with three antennas, and a sampling rate of 100Hz. It includes four sub-tasks: (1&2) User Identification and Biometrics Estimation, involving 30 participants who remained stationary for 100 seconds while their CSI signals were recorded at a distance of 1.6m; additional biometric attributes such as body fat and muscle rate were also provided; (3) Sign Language Recognition, in which one participant performed 10 American Sign Language digits (0–9), each lasting about 60 seconds, with the transmitter-receiver distance set to 0.6m; and (4) Fall Detection, where the same participant simulated falls at five different locations in the room, with each fall motion lasting 30 seconds and a 3.0m separation between transmitter and receiver.

IV. CHALLENGES AND FUTURE DIRECTIONS

A. Data, Data, Data

The scaling law, which involves training large-scale models with large-scale datasets, has proven its success since the advent of AlexNet [300], achieving remarkable breakthroughs in fields such as computer vision (CV), natural language processing (NLP), robotics, and science. Large-scale datasets like ImageNet [301], COCO [302], and Kinetics [303] have significantly accelerated advancements in these areas. In contrast, the field of Wi-Fi human sensing has not progressed as rapidly, despite the widespread adoption of deep learning methods. A key reason lies in the limited scale and diversity of available Wi-Fi sensing datasets.

Although researchers have made significant efforts to close this gap by collecting and releasing datasets like XRF55 [70] and Widar 3.0 [67], these datasets still suffer from constraints in terms of collection scenarios, action categories, and participant diversity. When compared to the scale of video, image, or text datasets, Wi-Fi sensing datasets lag behind by several orders of magnitude.

Collecting and annotating Wi-Fi sensing data is inherently time-consuming and labor-intensive. To address this bottleneck, synthetic data generation emerges as a promising solution. By producing large volumes of realistic data, synthetic methods can support the training of models with substantial parameters, potentially revolutionizing Wi-Fi sensing research. However, several open challenges remain to be addressed:

- 1) How to model the propagation of signals through people and environments? Can methods like ray-tracing and Fresnel zone models effectively simulate Wi-Fi signals' interactions with objects and people? How to enable modern approaches, such as diffusion models [262], Variational Autoencoders (VAEs) [304], Neural Radiance Fields (NeRF) [305], or 3D Gaussian Splatting [306] learn probabilistic mappings of signal propagation patterns from observed data?
- 2) How to construct diverse environments for data generation? Should we rely on manual modeling of environments, even though it is resource-intensive? Or should we leverage open-source tools like Unity, Unreal Engine, or Infinigen Indoors [307], which provide scalable solutions for generating dynamic, realistic environments tailored to Wi-Fi sensing scenarios?
- 3) How to synthesize diverse human body models? Is it more effective to use game engines like Unity or Unreal Engine to create diverse human models? Alternatively, could tools such as SMPL [308] or MANO [309] be utilized to extract human body models from large-scale video datasets for synthetic data generation?
- 4) How to bridge the gap between synthetic and real data? Could Generative Adversarial Networks (GANs) [252] help enhance the realism of synthetic features or adapt synthetic data to better match real-world characteristics? What role could domain adaptation and domain-invariant feature learning play in aligning synthetic and real data to improve model performance?

Addressing these challenges offers a pathway to creating realistic, diverse, and scalable synthetic Wi-Fi sensing datasets. By bridging the data gap, the Wi-Fi sensing field could achieve progress comparable to the rapid advancements seen in video, image, and text recognition, ultimately unlocking new frontiers for this promising domain.

B. Wi-Fi Sensing Foundation Model Pre-Training

Foundation models in vision and language, such as CLIP [310], GPT [311], and BERT [255], have demonstrated remarkable success in adapting to diverse downstream tasks. Similarly, Wi-Fi sensing encompasses a wide range of applications, including human activity recognition, indoor localization, presence detection, and pose estimation. These varied tasks make the development of a Wi-Fi sensing foundation model both promising and necessary. However, training such a model raises several critical open questions that must be addressed:

- 1) Should we utilize traditional architectures like CNNs and RNNs, or opt for Transformers [312], which have demonstrated strong performance across various domains? Alternatively, emerging architectures such as Mamba [313], known for their smaller parameter sizes, reduced memory consumption, and faster inference speeds, may also be viable options. Should we further tailor the architecture design to cater to different computational platforms, optimizing for specific hardware constraints and efficiency requirements?
- 2) How can unlabeled real-world data be incorporated effectively? While large-scale synthetic labeled data and small amounts of labeled real-world data may be used for training, how can we leverage large-scale unlabeled real-world data in the pre-training of the foundation model? Should this real-world data be transmitted to a central server for processing, or should edge computing be adopted to process data locally? Additionally, how can we coordinate with a large number of real-world users to ensure efficient data collection and processing while respecting privacy and computational constraints?
- 3) What self-supervised learning strategy is most suitable? Self-supervised learning can effectively leverage unlabeled data, but how should we design the proxy tasks? Should we employ contrastive learning strategies that bring positive sample pairs closer while pushing negative pairs apart? Or would a masking-then-reconstruction approach, as used in models like BERT [255] or MAE [314], be more appropriate for Wi-Fi sensing? Additionally, are there domain-specific proxy tasks that could better capture the unique spatiotemporal characteristics of Wi-Fi signals?
- 4) Wi-Fi sensing is significantly influenced by environmental factors and device configurations. Incorporating such information could enable the foundation model to reason more effectively about environmental changes and adapt to new scenarios. Should this integration be achieved through explicit embeddings of environmental and device parameters, or should the model be designed to infer these characteristics implicitly from the data?

Addressing these questions will be critical for developing a robust and generalizable Wi-Fi sensing foundation model that can serve as a backbone for various downstream applications.

C. When Wi-Fi Sensing Meets Large Multimodal Models

Beyond training Wi-Fi foundation models from scratch, as discussed in Section IV-B, another promising research direction is leveraging existing large multimodal models by fine-tuning them to process Wi-Fi sensing data. Large multimodal models, such as those trained on diverse combinations of images, text, and audio, have demonstrated impressive adaptability across various domains. By aligning Wi-Fi sensing data with these models, researchers may unlock new possibilities for enhanced understanding and application of Wi-Fi sensing technologies. However, integrating Wi-Fi data into such models raises several open questions and challenges:

- 1) What fine-tuning strategy is most effective? Fine-tuning large multimodal models requires balancing computational efficiency with task-specific performance improvements. Techniques like LoRA [315], adapters [316], or prompt-based fine-tuning [317] are popular in the NLP and vision domains. Should one of these strategies be adopted for Wi-Fi sensing, or is there a need for a novel approach tailored to the unique characteristics of Wi-Fi data? Moreover, how can we efficiently fine-tune large models with limited computational resources while ensuring high adaptability?
- 2) How can Wi-Fi data be aligned with the modalities handled by large multimodal models? Wi-Fi sensing data typically exists in time-series or signal-based formats, which differ significantly from image or text data commonly processed by multimodal models. Should the raw Wi-Fi data be transformed into spectrograms or other image-like representations for easier integration, or is it better to retain the time-series format and develop alignment techniques specific to such data? Furthermore, what pre-processing or feature extraction methods are necessary to achieve optimal performance when aligning Wi-Fi data with existing modalities?
- 3) How should domain-specific knowledge be incorporated into the model? Wi-Fi sensing encompasses a wealth of domain-specific knowledge, including signal propagation principles, communication protocols, e.g. IEEE 802.11 bf, and established research findings. Should this information be used to fine-tune models before fine-tuning on Wi-Fi signals, or would integrating Retrieval-Augmented Generation (RAG) [318] as an external database allow the model to access Wi-Fi knowledge on demand? How can this domain knowledge improve interpretability, efficiency, and overall performance?
- 4) What role does multimodal fusion play in Wi-Fi sensing? Large multimodal models excel at integrating and reasoning over diverse data sources. In Wi-Fi sensing, how can complementary modalities such as video, audio, or inertial measurements (e.g., IMU data) be effectively fused with Wi-Fi data? What techniques can ensure seamless fusion while addressing challenges like modality-

specific noise, synchronization issues, and computational overhead?

Addressing these challenges will advance the integration of Wi-Fi sensing with large multimodal models and push the boundaries of their application across various tasks and environments. This direction holds great potential for accelerating progress in Wi-Fi sensing by leveraging the capabilities of state-of-the-art AI models.

D. System Deployment and Service Models

As Wi-Fi sensing technologies advance and large multimodal models are integrated into Wi-Fi sensing applications, an essential next step involves addressing deployment and service models for these systems. Several critical questions arise when considering how to effectively and efficiently deploy such systems in real-world settings:

- 1) Large multimodal models often require high computational power and storage. Compression techniques like pruning [319], quantization [320], or knowledge distillation [321] can help balance performance and efficiency. How can these methods be tailored for different hardware (e.g., edge devices or mobile phones) to ensure speed without sacrificing too much performance?
- 2) How to manage network bandwidth, data traffic, and latency during operation? Network constraints, particularly with real-time data transmission, pose challenges. How can continuous data flow between edge devices and servers be optimized? Strategies like edge computing [322], which processes data locally, could reduce latency and bandwidth usage but introduce complexity in resource management and synchronization.
- 3) Should model updates be centralized or on-demand at the edge? Model updates can either be pushed centrally from a server or performed on-demand at the edge based on local needs. Centralized updates ensure consistency but may face bandwidth and computation constraints. Edge updates offer quick adaptability but can complicate coordination, version control, and synchronization.
- 4) What service and pricing strategies should be adopted? Deciding on the right service and pricing models is vital for commercialization. Should services be cloud-based, subscription-based, or pay-per-use? How can pricing be adapted based on usage, such as the number of devices, frequency of access, or task complexity? Should tiered services be offered, with basic models for simpler tasks and premium ones for more complex applications?

Addressing these questions will help define how Wi-Fi sensing services can be deployed and scaled efficiently in real-world applications, ultimately determining the practicality and success of Wi-Fi sensing systems across diverse industries and environments.

V. CONCLUSION

In this survey, we systematically reviewed and categorized Wi-Fi sensing generalization studies published between 2014 and 2025, following the end-to-end pipeline of Wi-Fi sensing

systems—spanning device deployment, model construction, and model deployment. We summarized key techniques proposed in each stage to address the challenges of domain variability. In addition, we provided a comprehensive overview of existing publicly available datasets, highlighting their domain diversity and applicability to generalization research.

By integrating methodological insights with data resources, this survey serves as a practical handbook for researchers aiming to advance the generalizability of Wi-Fi sensing systems. Beyond the current landscape, we also discussed future research directions, including synthetic dataset generation, pretraining large-scale perception models, integration with multimodal foundation models, and deployment-aware continual learning.

To further promote the development of Wi-Fi sensing, we have initiated the Sensing Dataset Platform (SDP: <http://www.sdp8.org>)—an open dataset and model sharing hub designed to foster collaboration between academia and industry.

REFERENCES

- [1] W. Jiang, C. Miao, F. Ma, S. Yao, Y. Wang, Y. Yuan, H. Xue, C. Song, X. Ma, D. Koutsonikolas, W. Xu, and L. Su, “Towards environment independent device free human activity recognition,” in *MobiCom*, 2018, pp. 289–304.
- [2] W. Wang, A. X. Liu, M. Shahzad, K. Ling, and S. Lu, “Understanding and modeling of wifi signal based human activity recognition,” in *MobiCom*, 2015, pp. 65–76.
- [3] S. Tan, L. Zhang, Z. Wang, and J. Yang, “Multitrack: Multi-user tracking and activity recognition using commodity wifi,” in *CHI*, 2019, pp. 1–12.
- [4] H. Zhu, F. Xiao, L. Sun, R. Wang, and P. Yang, “R-ttwd: Robust device-free through-the-wall detection of moving human with wifi,” *IEEE JASAC*, vol. 35, no. 5, pp. 1090–1103, 2017.
- [5] Y. Wang, J. Liu, Y. Chen, M. Gruteser, J. Yang, and H. Liu, “E-eyes: Device-free location-oriented activity identification using fine-grained wifi signatures,” in *MobiCom*, 2014, pp. 617–628.
- [6] Z. Chen, L. Zhang, C. Jiang, Z. Cao, and W. Cui, “Wifi csi based passive human activity recognition using attention based blstm,” *IEEE TMC*, vol. 18, no. 11, pp. 2714–2724, 2018.
- [7] F. Adib and D. Katabi, “See through walls with wifi!” in *ACM SIGCOMM*, 2013, pp. 75–86.
- [8] M. Li, Y. Meng, J. Liu, H. Zhu, X. Liang, Y. Liu, and N. Ruan, “When csi meets public wifi: Inferring your mobile phone password via wifi signals,” in *ACM CCS*, 2016, pp. 1068–1079.
- [9] Q. Pu, S. Gupta, S. Gollakota, and S. Patel, “Whole-home gesture recognition using wireless signals,” in *MobiCom*, 2013, pp. 27–38.
- [10] H. Li, W. Yang, J. Wang, Y. Xu, and L. Huang, “Wifinger: Talk to your smart devices with finger-grained gesture,” in *UBICOMP*, 2016, pp. 250–261.
- [11] K. Ali, A. X. Liu, W. Wang, and M. Shahzad, “Keystroke recognition using wifi signals,” in *MobiCom*, 2015, pp. 90–102.
- [12] R. H. Venkatnarayan, G. Page, and M. Shahzad, “Multi-user gesture recognition using wifi,” in *MobiSys*, 2018, pp. 401–413.
- [13] H. Abdelnasser, M. Youssef, and K. A. Harras, “Wigest: A ubiquitous wifi-based gesture recognition system,” in *INFOCOM*. IEEE, 2015, pp. 1472–1480.
- [14] Y. Ma, G. Zhou, S. Wang, H. Zhao, and W. Jung, “Signfi: Sign language recognition using wifi,” *IMWUT*, vol. 2, no. 1, pp. 1–21, 2018.
- [15] F. Wang, J. Feng, Y. Zhao, X. Zhang, S. Zhang, and J. Han, “Joint activity recognition and indoor localization with wifi fingerprints,” *Ieee Access*, vol. 7, pp. 80 058–80 068, 2019.
- [16] L. Sun, S. Sen, D. Koutsonikolas, and K.-H. Kim, “Widraw: Enabling hands-free drawing in the air on commodity wifi devices,” in *MobiCom*, 2015, pp. 77–89.
- [17] X. Li, S. Li, D. Zhang, J. Xiong, Y. Wang, and H. Mei, “Dynamic-music: Accurate device-free indoor localization,” in *UBICOMP*, 2016, pp. 196–207.
- [18] Y. Xie, Z. Li, and M. Li, “Precise power delay profiling with commodity wifi,” in *MobiCom*, 2015, pp. 53–64.
- [19] D. Vasisht, S. Kumar, and D. Katabi, “{Decimeter-Level} localization with a single {WiFi} access point,” in *NSDI*, 2016, pp. 165–178.
- [20] K. Qian, C. Wu, Z. Yang, Y. Liu, and K. Jamieson, “Widar: Decimeter-level passive tracking via velocity monitoring with commodity wi-fi,” in *ACM MobiHoc*, 2017, pp. 1–10.
- [21] X. Li, D. Zhang, Q. Lv, J. Xiong, S. Li, Y. Zhang, and H. Mei, “Indotrack: Device-free indoor human tracking with commodity wi-fi,” *IMWUT*, vol. 1, no. 3, pp. 1–22, 2017.
- [22] Y. Xie, J. Xiong, M. Li, and K. Jamieson, “md-track: Leveraging multi-dimensionality for passive indoor wi-fi tracking,” in *MobiCom*, 2019, pp. 1–16.
- [23] K. Qian, C. Wu, Y. Zhang, G. Zhang, Z. Yang, and Y. Liu, “Widar2.0: Passive human tracking with a single wi-fi link,” in *MobiSys*, 2018, pp. 350–361.
- [24] M. Kotaru, K. Joshi, D. Bharadia, and S. Katti, “Spotfi: Decimeter level localization using wifi,” in *Proceedings of the ACM Conference on Special Interest Group on Data Communication*, 2015, pp. 269–282.
- [25] B. Korany, C. R. Karanam, H. Cai, and Y. Mostofi, “Xmodal-id: Using wifi for through-wall person identification from candidate video footage,” in *MobiCom*, 2019, pp. 1–15.
- [26] F. Wang, Z. Li, and J. Han, “Continuous user authentication by contactless wireless sensing,” *IoT-J*, vol. 6, no. 5, pp. 8323–8331, 2019.
- [27] F. Wang, J. Han, F. Lin, and K. Ren, “Wipin: Operation-free passive person identification using wi-fi signals,” in *GLOBECOM*. IEEE, 2019, pp. 1–6.
- [28] C. Shi, J. Liu, H. Liu, and Y. Chen, “Smart user authentication through actuation of daily activities leveraging wifi-enabled iot,” in *ACM MobiHoc*, 2017, pp. 1–10.
- [29] Y. Zeng, P. H. Pathak, and P. Mohapatra, “Wiwho: Wifi-based person identification in smart spaces,” in *ACM/IEEE IPSN*, 2016, pp. 1–12.
- [30] Y. Zhang, Y. Zheng, G. Zhang, K. Qian, C. Qian, and Z. Yang, “Gaitid: Robust wi-fi based gait recognition,” in *WASA*. Springer, 2020, pp. 730–742.
- [31] W. Wang, A. X. Liu, and M. Shahzad, “Gait recognition using wifi signals,” in *UBICOMP*, 2016, pp. 363–373.
- [32] Y. Zeng, D. Wu, J. Xiong, J. Liu, Z. Liu, and D. Zhang, “Multisense: Enabling multi-person respiration sensing with commodity wifi,” *IMWUT*, vol. 4, no. 3, pp. 1–29, 2020.
- [33] X. Wang, C. Yang, and S. Mao, “Tensorbeat: Tensor decomposition for monitoring multiperson breathing beats with commodity wifi,” *ACM Transactions on Intelligent Systems and Technology*, vol. 9, no. 1, pp. 1–27, 2017.
- [34] Y. Zeng, D. Wu, R. Gao, T. Gu, and D. Zhang, “Fullbreathe: Full human respiration detection exploiting complementarity of csi phase and amplitude of wifi signals,” *IMWUT*, vol. 2, no. 3, pp. 1–19, 2018.
- [35] H. Wang, D. Zhang, J. Ma, Y. Wang, Y. Wang, D. Wu, T. Gu, and B. Xie, “Human respiration detection with commodity wifi devices: Do user location and body orientation matter?” in *UBICOMP*, 2016, pp. 25–36.
- [36] X. Zheng, J. Wang, L. Shangguan, Z. Zhou, and Y. Liu, “Smokey: Ubiquitous smoking detection with commercial wifi infrastructures,” in *INFOCOM*. IEEE, 2016, pp. 1–9.
- [37] Y. Zeng, D. Wu, J. Xiong, E. Yi, R. Gao, and D. Zhang, “Farsense: Pushing the range limit of wifi-based respiration sensing with csi ratio of two antennas,” *IMWUT*, vol. 3, no. 3, pp. 1–26, 2019.
- [38] H. Wang, D. Zhang, Y. Wang, J. Ma, Y. Wang, and S. Li, “Rt-fall: A real-time and contactless fall detection system with commodity wifi devices,” *IEEE TMC*, vol. 16, no. 2, pp. 511–526, 2016.
- [39] S. Palipana, D. Rojas, P. Agrawal, and D. Pesch, “Falldefi: Ubiquitous fall detection using commodity wi-fi devices,” *IMWUT*, vol. 1, no. 4, pp. 1–25, 2018.
- [40] Y. Wang, K. Wu, and L. M. Ni, “Wifall: Device-free fall detection by wireless networks,” *IEEE TMC*, vol. 16, no. 2, pp. 581–594, 2016.
- [41] J. Ding and Y. Wang, “A wifi-based smart home fall detection system using recurrent neural network,” *IEEE Transactions on Consumer Electronics*, vol. 66, no. 4, pp. 308–317, 2020.
- [42] Y. Hu, F. Zhang, C. Wu, B. Wang, and K. R. Liu, “Defall: Environment-independent passive fall detection using wifi,” *IoT-J*, vol. 9, no. 11, pp. 8515–8530, 2021.
- [43] W. Jiang, H. Xue, C. Miao, S. Wang, S. Lin, C. Tian, S. Murali, H. Hu, Z. Sun, and L. Su, “Towards 3d human pose construction using wifi,” in *MobiCom*, 2020, pp. 1–14.
- [44] F. Wang, S. Panev, Z. Dai, J. Han, and D. Huang, “Can wifi estimate person pose?” *arXiv preprint arXiv:1904.00277*, 2019.
- [45] F. Wang, S. Zhou, S. Panev, J. Han, and D. Huang, “Person-in-wifi: Fine-grained person perception using wifi,” in *ICCV*, 2019, pp. 5452–5461.

[46] Y. Ren, Z. Wang, Y. Wang, S. Tan, Y. Chen, and J. Yang, "Gopose: 3d human pose estimation using wifi," *IMWUT*, vol. 6, no. 2, pp. 1–25, 2022.

[47] Y. Wang, Y. Ren, and J. Yang, "Multi-subject 3d human mesh construction using commodity wifi," *IMWUT*, vol. 8, no. 1, pp. 1–25, 2024.

[48] Y. Wang, Y. Ren, Y. Chen, and J. Yang, "Wi-mesh: A wifi vision-based approach for 3d human mesh construction," in *SenSys*, 2022, pp. 362–376.

[49] B. Qian, X. Wei, K. Yan, and F. Wang, "From sparse to dense: Learning to construct 3d human meshes from wifi," 2023.

[50] K. Yan, F. Wang, B. Qian, H. Ding, J. Han, and X. Wei, "Person-in-wifi 3d: End-to-end multi-person 3d pose estimation with wi-fi," in *CVPR*, 2024, pp. 969–978.

[51] H. Zou, Y. Zhou, J. Yang, W. Gu, L. Xie, and C. Spanos, "Freecount: Device-free crowd counting with commodity wifi," in *GLOBECOM*. IEEE, 2017, pp. 1–6.

[52] H. Zou, Y. Zhou, J. Yang, and C. J. Spanos, "Device-free occupancy detection and crowd counting in smart buildings with wifi-enabled iot," *Energy and Buildings*, vol. 174, pp. 309–322, 2018.

[53] H. Choi, M. Fujimoto, T. Matsui, S. Misaki, and K. Yasumoto, "Wi-cal: Wifi sensing and machine learning based device-free crowd counting and localization," *IEEE Access*, vol. 10, pp. 24 395–24 410, 2022.

[54] H. Jiang, S. Chen, Z. Xiao, J. Hu, J. Liu, and S. Dusdar, "Pa-count: passenger counting in vehicles using wi-fi signals," *IEEE TMC*, vol. 23, no. 4, pp. 2684–2697, 2023.

[55] W. Xi, J. Zhao, X.-Y. Li, K. Zhao, S. Tang, X. Liu, and Z. Jiang, "Electronic frog eye: Counting crowd using wifi," in *INFOCOM*. IEEE, 2014, pp. 361–369.

[56] S. Tan, Y. Ren, J. Yang, and Y. Chen, "Commodity wifi sensing in ten years: Status, challenges, and opportunities," *IoT-J*, vol. 9, no. 18, pp. 17 832–17 843, 2022.

[57] S. M. Hernandez and E. Bulut, "Wifi sensing on the edge: Signal processing techniques and challenges for real-world systems," *IEEE Communications Surveys & Tutorials*, vol. 25, no. 1, pp. 46–76, 2022.

[58] R. Zhang, X. Jing, S. Wu, C. Jiang, J. Mu, and F. R. Yu, "Device-free wireless sensing for human detection: The deep learning perspective," *IoT-J*, vol. 8, no. 4, pp. 2517–2539, 2020.

[59] Y. Ma, G. Zhou, and S. Wang, "Wifi sensing with channel state information: A survey," *ACM Computing Surveys*, vol. 52, no. 3, pp. 1–36, 2019.

[60] J. Liu, H. Liu, Y. Chen, Y. Wang, and C. Wang, "Wireless sensing for human activity: A survey," *IEEE Communications Surveys & Tutorials*, vol. 22, no. 3, pp. 1629–1645, 2019.

[61] C. Li, Z. Cao, and Y. Liu, "Deep ai enabled ubiquitous wireless sensing: A survey," *ACM Computing Surveys*, vol. 54, no. 2, pp. 1–35, 2021.

[62] S. Yousefi, H. Narui, S. Dayal, S. Ermon, and S. Valaee, "A survey on behavior recognition using wifi channel state information," *IEEE Communications Magazine*, vol. 55, no. 10, pp. 98–104, 2017.

[63] Y. Qin, S. Sigg, S. Pan, and Z. Li, "Direction-agnostic gesture recognition system using commercial wifi devices," *Computer Communications*, vol. 216, pp. 34–44, 2024.

[64] Y. Qin, S. Pan, and Z. Li, "Cross-domain extendable gesture recognition system using wifi signals," *Electronics Letters*, vol. 59, no. 16, p. e12931, 2023.

[65] F. Wang, W. Gong, and J. Liu, "On spatial diversity in wifi-based human activity recognition: A deep learning-based approach," *IoT-J*, vol. 6, no. 2, pp. 2035–2047, 2018.

[66] N. Bahadori, J. Ashdown, and F. Restuccia, "Rewis: Reliable wi-fi sensing through few-shot multi-antenna multi-receiver csi learning," in *WoWMoM*. IEEE, 2022, pp. 50–59.

[67] Y. Zheng, Y. Zhang, K. Qian, G. Zhang, Y. Liu, C. Wu, and Z. Yang, "Zero-effort cross-domain gesture recognition with wi-fi," in *MobiSys*, 2019, pp. 313–325.

[68] R. Xiao, J. Liu, J. Han, and K. Ren, "Onefi: One-shot recognition for unseen gesture via cots wifi," in *SenSys*, 2021, pp. 206–219.

[69] D. Wu, Y. Zeng, R. Gao, S. Li, Y. Li, R. C. Shah, H. Lu, and D. Zhang, "Witraj: Robust indoor motion tracking with wifi signals," *IEEE TMC*, vol. 22, no. 5, pp. 3062–3078, 2021.

[70] F. Wang, Y. Lv, M. Zhu, H. Ding, and J. Han, "Xrf55: A radio frequency dataset for human indoor action analysis," *IMWUT*, vol. 8, no. 1, pp. 1–34, 2024.

[71] Y. Zhang, Y. Yin, Y. Wang, J. Ai, and D. Wu, "Csi-based location-independent human activity recognition with parallel convolutional networks," *Computer Communications*, vol. 197, pp. 87–95, 2023.

[72] J. Yang, H. Huang, Y. Zhou, X. Chen, Y. Xu, S. Yuan, H. Zou, C. X. Lu, and L. Xie, "Mm-fi: Multi-modal non-intrusive 4d human dataset for versatile wireless sensing," *NeurIPS*, vol. 36, 2024.

[73] G. Zhu, Y. Hu, W. Gao, W.-H. Wang, B. Wang, and K. Liu, "Csi-bench: A large-scale in-the-wild dataset for multi-task wifi sensing," *arXiv preprint arXiv:2505.21866*, 2025.

[74] Y. Lu, S. Lv, and X. Wang, "Towards location independent gesture recognition with commodity wifi devices," *Electronics*, vol. 8, no. 10, p. 1069, 2019.

[75] R. Zhou, Z. Gong, K. Tang, B. Zhou, and Y. Cheng, "Device-free cross location activity recognition via semi-supervised deep learning," *Neural Computing and Applications*, vol. 34, no. 12, pp. 10 189–10 203, 2022.

[76] J. Yang, Y. Liu, Y. Wu, P. Yang, and Z. Liu, "Gait-enhance: Robust gait recognition of complex walking patterns based on wifi csi," in *Smart World Congress*. IEEE, 2023, pp. 1–9.

[77] H. Zhuo, X. Wu, Q. Zhong, and H. Zhang, "Position-free breath detection during sleep via commodity wifi," *IEEE Sensors Journal*, 2023.

[78] F. Abuhoureyah, S. K. Swee, and W. Y. Chiew, "Multi-user human activity recognition through adaptive location-independent wifi signal characteristics," *IEEE Access*, 2024.

[79] W. Meng, X. Chen, W. Cui, and J. Guo, "Wihgr: A robust wifi-based human gesture recognition system via sparse recovery and modified attention-based bgru," *IoT-J*, vol. 9, no. 12, pp. 10 272–10 282, 2021.

[80] J. Huang, B. Liu, C. Miao, Y. Lu, Q. Zheng, Y. Wu, J. Liu, L. Su, and C. W. Chen, "Phaseanti: An anti-interference wifi-based activity recognition system using interference-independent phase component," *IEEE TMC*, vol. 22, no. 5, pp. 2938–2954, 2021.

[81] R. Gao, W. Li, Y. Xie, E. Yi, L. Wang, D. Wu, and D. Zhang, "Towards robust gesture recognition by characterizing the sensing quality of wifi signals," *IMWUT*, vol. 6, no. 1, pp. 1–26, 2022.

[82] J. Zhang, Y. Li, H. Xiong, D. Dou, C. Miao, and D. Zhang, "Handgest: Hierarchical sensing for robust-in-the-air handwriting recognition with commodity wifi devices," *IoT-J*, vol. 9, no. 19, pp. 19 529–19 544, 2022.

[83] X. Yu, T. Jiang, X. Ding, Z. Yao, X. Zhou, and Y. Zhong, "Towards position-independent gesture recognition based on wifi by subcarrier selection and gesture code," in *WCNC*. IEEE, 2023, pp. 1–6.

[84] Y. Zhang, Q. Liu, Y. Wang, and G. Yu, "Csi-based location-independent human activity recognition using feature fusion," *IEEE TIM*, vol. 71, pp. 1–12, 2022.

[85] C. Peng, L. Gui, B. Sheng, Z. Guo, and F. Xiao, "Rosefi: A robust sedentary behavior monitoring system with commodity wifi devices," *IEEE TMC*, 2023.

[86] X. Wang, A. Yu, K. Niu, W. Shi, J. Wang, Z. Yao, R. C. Shah, H. Lu, and D. Zhang, "Understanding the diffraction model in static multipath-rich environments for wifi sensing system design," *IEEE TMC*, 2024.

[87] X. Ding, X. Yu, Y. Zhong, W. Xie, B. Cai, M. You, and T. Jiang, "Robust gesture recognition method toward intelligent environment using wi-fi signals," *Measurement*, vol. 231, p. 114525, 2024.

[88] M. Peng, X. Fu, H. Zhao, Y. Wang, and C. Kai, "Likey: Location-independent keystroke recognition on numeric keypads using wifi signal," *Computer Networks*, vol. 245, p. 110354, 2024.

[89] Q. Bu, G. Yang, J. Feng, and X. Ming, "Wi-fi based gesture recognition using deep transfer learning," in *SmartWorld, Ubiquitous Intelligence & Computing, Advanced & Trusted Computing, Scalable Computing & Communications, Cloud & Big Data Computing, Internet of People and Smart City Innovation*. IEEE, 2018, pp. 590–595.

[90] C. Zhang, W. Jiao, and W. Du, "Enhancing human activity recognition performance in small-sample wi-fi sensing using data augmentation methods," in *ICCT*. IEEE, 2023, pp. 473–478.

[91] F. Meneghelli, D. Garlisi, N. Dal Fabbro, I. Tinnirello, and M. Rossi, "Sharp: Environment and person independent activity recognition with commodity ieee 802.11 access points," *IEEE TMC*, vol. 22, no. 10, pp. 6160–6175, 2022.

[92] L. Zhao, R. Xiao, J. Liu, and J. Han, "One is enough: Enabling one-shot device-free gesture recognition with cots wifi," in *INFOCOM*. IEEE, 2024, pp. 1231–1240.

[93] Y. Yin, Z. Zhang, X. Yang, F. Yan, and Q. Niu, "Towards fully domain-independent gesture recognition using cots wifi device," *Electronics Letters*, vol. 57, no. 5, pp. 232–234, 2021.

[94] C. Feng, N. Wang, Y. Jiang, X. Zheng, K. Li, Z. Wang, and X. Chen, "Wi-learner: Towards one-shot learning for cross-domain wi-fi based gesture recognition," *IMWUT*, vol. 6, no. 3, pp. 1–27, 2022.

[95] K. Niu, F. Zhang, X. Wang, Q. Lv, H. Luo, and D. Zhang, "Understanding wifi signal frequency features for position-independent gesture sensing," *IEEE TMC*, vol. 21, no. 11, pp. 4156–4171, 2021.

[96] J. Chen, S. Bi, X.-H. Lin, and Z. Quan, "Lager: Label-free domain-adaptive wireless gesture recognition via latent feature alignment and augmentation," *IoT-J*, vol. 11, no. 23, pp. 37 928–37 941, 2024.

[97] S. Li, Z. Liu, Q. Lv, Y. Zou, Y. Zhang, and D. Zhang, "Wilife: Long-term daily status monitoring and habit mining of the elderly leveraging ubiquitous wi-fi signals," *ACM Transactions on Computing for Healthcare*.

[98] B. van Berlo, C. Oerlemans, F. L. Marogna, T. Ozcelebi, and N. Meratnia, "Mini-batch alignment: A deep-learning model for domain factor-independent feature extraction for wi-fi-csi data," *Sensors*, vol. 23, no. 23, p. 9534, 2023.

[99] B. van Berlo, T. Ozcelebi, and N. Meratnia, "Insights on mini-batch alignment for wifi-csi data domain factor independent feature extraction," in *International Conference on Pervasive Computing and Communications Workshops and other Affiliated Event*. IEEE, 2022, pp. 527–532.

[100] B.-B. Zhang, D. Zhang, Y. Hu, and Y. Chen, "Unsupervised domain adaptation for wifi gesture recognition," in *WCNC*. IEEE, 2023, pp. 1–6.

[101] M. Yang, H. Zhu, R. Zhu, F. Wu, L. Yin, and Y. Yang, "Witransformer: A novel robust gesture recognition sensing model with wifi," *Sensors*, vol. 23, no. 5, p. 2612, 2023.

[102] W. Shi, M. Duan, H. He, L. Lin, C. Yang, C. Li, and J. Zhao, "Location adaptive motion recognition based on wi-fi feature enhancement," *Applied Sciences*, vol. 13, no. 3, p. 1320, 2023.

[103] I. Bulugu, "Gesture recognition system based on cross-domain csi extracted from wi-fi devices combined with the 3d cnn," *Signal, Image and Video Processing*, vol. 17, no. 6, pp. 3201–3209, 2023.

[104] G. Chi, G. Zhang, X. Ding, Q. Ma, Z. Yang, Z. Du, H. Xiao, and Z. Liu, "Xfall: Domain adaptive wi-fi-based fall detection with cross-modal supervision," *IEEE JASAC*, 2024.

[105] R. Gao, M. Zhang, J. Zhang, Y. Li, E. Yi, D. Wu, L. Wang, and D. Zhang, "Towards position-independent sensing for gesture recognition with wi-fi," *IMWUT*, vol. 5, no. 2, pp. 1–28, 2021.

[106] C. Shi, J. Liu, N. Borodinov, B. Leao, and Y. Chen, "Towards environment-independent behavior-based user authentication using wifi," in *MASS*. IEEE, 2020, pp. 666–674.

[107] Y. Wang, Y. Tian, and R. Peng, "Position and orientation independent wireless gesture recognition," in *WCSP*. IEEE, 2022, pp. 466–471.

[108] D. Wu, D. Zhang, C. Xu, Y. Wang, and H. Wang, "Widir: Walking direction estimation using wireless signals," in *UBICOMP*, 2016, pp. 351–362.

[109] H. Wang, D. Zhang, J. Ma, Y. Wang, Y. Wang, D. Wu, T. Gu, and B. Xie, "Human respiration detection with commodity wifi devices: Do user location and body orientation matter?" in *UBICOMP*, 2016, pp. 25–36.

[110] L. Zhang, C. Wang, M. Ma, and D. Zhang, "Widigr: Direction-independent gait recognition system using commercial wi-fi devices," *IoT-J*, vol. 7, no. 2, pp. 1178–1191, 2019.

[111] L. Zhang, C. Wang, and D. Zhang, "Wi-pigr: Path independent gait recognition with commodity wi-fi," *IEEE TMC*, vol. 21, no. 9, pp. 3414–3427, 2021.

[112] F. Zhang, C. Wu, B. Wang, H.-Q. Lai, Y. Han, and K. R. Liu, "Widetect: Robust motion detection with a statistical electromagnetic model," *IMWUT*, vol. 3, no. 3, pp. 1–24, 2019.

[113] G. Zhu, B. Wang, W. Gao, Y. Hu, C. Wu, and K. R. Liu, "Wifi-based robust human and non-human motion recognition with deep learning," in *PerCom Workshops*. IEEE, 2024, pp. 769–774.

[114] Y. Li, T. Jiang, X. Ding, and Y. Wang, "Location-free csi based activity recognition with angle difference of arrival," in *WCNC*. IEEE, 2020, pp. 1–6.

[115] Z. Han, Z. Lu, Z. Hu, Y. Chen, and X. Wen, "On position-independency passive gesture tracking with commodity wi-fi," *IEEE Sensors Journal*, vol. 23, no. 14, pp. 16264–16275, 2023.

[116] Y. Ren and J. Yang, "Robust person identification: A wifi vision-based approach," *arXiv preprint arXiv:2210.00127*, 2022.

[117] Z. Wang, S. Chen, W. Yang, and Y. Xu, "Environment-independent wi-fi human activity recognition with adversarial network," in *ICASSP*. IEEE, 2021, pp. 3330–3334.

[118] L. Sheng, Y. Chen, S. Ning, S. Wang, B. Lian, and Z. Wei, "Dahar: Dual adversarial network for environment-independent wifi human activity recognition," *Pervasive and Mobile Computing*, vol. 96, p. 101850, 2023.

[119] L. Zhang, W. Cui, B. Li, Z. Chen, M. Wu, and T. S. Gee, "Privacy-preserving cross-environment human activity recognition," *IEEE Transactions on Cybernetics*, vol. 53, no. 3, pp. 1765–1775, 2021.

[120] Z. Zhou, F. Wang, and W. Gong, "i-sample: Augment domain adversarial adaptation models for wifi-based har," *ACM ToSN*, vol. 20, no. 2, pp. 1–20, 2024.

[121] H. Zou, J. Yang, Y. Zhou, and C. J. Spanos, "Joint adversarial domain adaptation for resilient wifi-enabled device-free gesture recognition," in *ICMLA*. IEEE, 2018, pp. 202–207.

[122] X. Li, L. Chang, F. Song, J. Wang, X. Chen, Z. Tang, and Z. Wang, "Crossgr: Accurate and low-cost cross-target gesture recognition using wi-fi," *IMWUT*, vol. 5, no. 1, pp. 1–23, 2021.

[123] H. Zhang, Z. Zhou, and W. Gong, "Wi-adaptor: Fine-grained domain adaptation in wifi-based activity recognition," in *GLOBECOM*. IEEE, 2021, pp. 1–6.

[124] W. Jiang, C. Miao, F. Ma, S. Yao, Y. Wang, Y. Yuan, H. Xue, C. Song, X. Ma, D. Koutsonikolas, W. Xu, and L. Su, "Towards environment independent device free human activity recognition," in *MobiCom*, 2018, pp. 289–304.

[125] A. Khattak and A. Khan, "Cross-location activity recognition using adversarial learning," in *SOICT*, 2022, pp. 59–65.

[126] F. Wang, J. Liu, and W. Gong, "Wicar: Wifi-based in-car activity recognition with multi-adversarial domain adaptation," in *IWQoS*, 2019, pp. 1–10.

[127] X. Zhang, Y. Feng, J. Huang, H. Yan, P. Zhao, J. Liu, T. Liu, M. Li, Z. Liu, and B. Liu, "Objective gesture recognition based on wifi," *Authorea Preprints*, 2024.

[128] A. Zinys, B. van Berlo, and N. Meratnia, "A domain-independent generative adversarial network for activity recognition using wifi csi data," *Sensors*, vol. 21, no. 23, p. 7852, 2021.

[129] J. Strohmayer, R. Sterzinger, M. Wödlinger, and M. Kampel, "Datta: Domain-adversarial test-time adaptation for cross-domain wifi-based human activity recognition," *arXiv preprint arXiv:2411.13284*, 2024.

[130] S. Liu, Z. Chen, M. Wu, C. Liu, and L. Chen, "WISR: Wireless domain generalization based on style randomization," *IEEE TMC*, 2023.

[131] W. Yang, X. Jiawei, W. Ao, X. Huijuan, Z. Chuanxin, and J. Yimu, "Domain-generalization human activity recognition model based on csi instance normalization," *Journal on Communication/Tongxin Xuebao*, vol. 45, no. 6, 2024.

[132] B. v. Berlo, R. Verhoeven, and N. Meratnia, "Use of domain labels during pre-training for domain-independent wifi-csi gesture recognition," *Sensors*, vol. 23, no. 22, p. 9233, 2023.

[133] S. Zhou, L. Guo, Z. Lu, X. Wen, W. Zheng, and Y. Wang, "Subject-independent human pose image construction with commodity wi-fi," in *IEEE ICC*, 2021, pp. 1–6.

[134] D. Yan, P. Yang, F. Shang, F. Han, Y. Yan, and X.-Y. Li, "freegait: Liberalizing wireless-based gait recognition to mitigate non-gait human behaviors," in *MobiHoc*, 2024, pp. 241–250.

[135] H. Li, X. Chen, J. Wang, D. Wu, and X. Liu, "Dafi: Wifi-based device-free indoor localization via domain adaptation," *IMWUT*, vol. 5, no. 4, pp. 1–21, 2021.

[136] X. Chen, H. Li, C. Zhou, X. Liu, D. Wu, and G. Dudek, "Fidora: Robust wifi-based indoor localization via unsupervised domain adaptation," *IoT-J*, vol. 9, no. 12, pp. 9872–9888, 2022.

[137] A. Gretton, K. Borgwardt, M. Rasch, B. Schölkopf, and A. Smola, "A kernel method for the two-sample-problem," *NeurIPS*, vol. 19, 2006.

[138] Y. Zhou, J. Yang, H. Huang, and L. Xie, "Adapose: Towards cross-site device-free human pose estimation with commodity wifi," *IoT-J*, 2024.

[139] X. Rao, L. Qin, Y. Yi, J. Liu, G. Lei, and Y. Cao, "A novel adaptive device-free passive indoor fingerprinting localization under dynamic environment," *IEEE TNSM*, 2024.

[140] H. Kang, Q. Zhang, and Q. Huang, "Context-aware wireless-based cross-domain gesture recognition," *IoT-J*, vol. 8, no. 17, pp. 13 503–13 515, 2021.

[141] Y. Liang, W. Wu, H. Li, F. Han, Z. Liu, P. Xu, X. Lian, and X. Chen, "WiAi-id: Wi-fi-based domain adaptation for appearance-independent passive person identification," *IoT-J*, vol. 11, no. 1, pp. 1012–1027, 2023.

[142] S. Zhang, T. Jiang, X. Ding, X. Zhou, and Y. Zhong, "Device-free cross-environment human action recognition using wi-fi signals," in *International Conference on Artificial Intelligence in China*. Springer, 2023, pp. 141–151.

[143] S. Mehryar, "A domain adaptation framework for human activity monitoring using passive wi-fi sensing," in *ICCCMLA*. IEEE, 2023, pp. 263–268.

[144] R. Zhou, H. Hou, Z. Gong, Z. Chen, K. Tang, and B. Zhou, "Adaptive device-free localization in dynamic environments through adaptive neural networks," *IEEE Sensors Journal*, vol. 21, no. 1, pp. 548–559, 2020.

[145] Z. Xiao, S. Zhou, X. Wen, S. Ling, and X. Yang, "Pattern-independent human gait identification with commodity wifi," in *WCNC*. IEEE, 2024, pp. 1–6.

[146] G. Kang, L. Jiang, Y. Yang, and A. G. Hauptmann, "Contrastive adaptation network for unsupervised domain adaptation," in *CVPR*, 2019, pp. 4893–4902.

[147] W. Cui, K. Wu, M. Wu, X. Li, and Z. Chen, "Wicau: Comprehensive partial adaptation with uncertainty-aware for wifi-based cross-environment activity recognition," *IEEE TIM*, vol. 73, pp. 1–10, 2024.

[148] W. Jiao, C. Zhang, W. Du, and S. Ma, "Wisda: Subdomain adaptation human activity recognition method using wi-fi signals," *IEEE TMC*, 2024.

[149] K. Gong, Y. Gao, and W. Dong, "Privacy-preserving and cross-domain human sensing by federated domain adaptation with semantic knowledge correction," *IMWUT*, vol. 8, no. 1, pp. 1–26, 2024.

[150] B. Sheng, R. Han, H. Cai, F. Xiao, L. Gui, and Z. Guo, "Cdfi: Cross-domain action recognition using wifi signals," *IEEE TMC*, 2024.

[151] X. Zhan and Z. Wu, "Indoor positioning based on channel state information and deep learning domain adaptation," in *ICCAID*, vol. 13105. SPIE, 2024, pp. 918–930.

[152] D. Wang, J. Yang, W. Cui, L. Xie, and S. Sun, "Airfi: empowering wifi-based passive human gesture recognition to unseen environment via domain generalization," *IEEE TMC*, vol. 23, no. 2, pp. 1156–1168, 2022.

[153] X. Ding, T. Jiang, Y. Li, W. Xue, and Y. Zhong, "Device-free location-independent human activity recognition using transfer learning based on cnn," in *ICC Workshops*. IEEE, 2020, pp. 1–6.

[154] J. Zhang, Z. Chen, C. Luo, B. Wei, S. S. Kanhere, and J. Li, "Metaganfi: Cross-domain unseen individual identification using wifi signals," *IMWUT*, vol. 6, no. 3, pp. 1–21, 2022.

[155] H. Zhang, X. Chen, and S. Chen, "Cross-domain wi-fi sign language recognition with gans," in *ICCBN*, 2022, pp. 60–65.

[156] Y. Mao, Z. Guo, B. Sheng, L. Gui, and F. Xiao, "Wi-cro: Wifi-based cross domain activity recognition via modified gan," *IEEE TVT*, 2024.

[157] C. Xiao, Y. Lei, C. Liu, and J. Wu, "Mean teacher-based cross-domain activity recognition using wifi signals," *IoT-J*, vol. 10, no. 14, pp. 12 787–12 797, 2023.

[158] J. Zhang, Z. Tang, M. Li, D. Fang, P. Nurmi, and Z. Wang, "Crosssense: Towards cross-site and large-scale wifi sensing," in *MobiCom*, 2018, pp. 305–320.

[159] Y. Sugimoto, H. Rizk, A. Uchiyama, and H. Yamaguchi, "Towards environment-independent activity recognition using wi-fi csi with an encoder-decoder network," in *BodySys*, 2023, pp. 13–18.

[160] Y. Zhang, A. Cheng, B. Chen, Y. Wang, and L. Jia, "A location-independent human activity recognition method based on csi: System, architecture, implementation," *IEEE TMC*, 2023.

[161] M. T. Islam and S. Nirjon, "Wi-fringe: Leveraging text semantics in wifi csi-based device-free named gesture recognition," in *DCOSS*. IEEE, 2020, pp. 35–42.

[162] H. Zhang, Y. Ren, H. Yuan, J. Zhang, and Y. Shen, "Wi-chat: Large language model powered wi-fi sensing," *arXiv preprint arXiv:2502.12421*, 2025.

[163] I. Nirmal, A. Khamis, M. Hassan, W. Hu, R. Li, and A. Kalyanaraman, "Wifi2radar: Orientation-independent single-receiver wifi sensing via wifi to radar translation," *IoT-J*, vol. 11, no. 9, pp. 15 750–15 766, 2024.

[164] I. Elujide, C. Feng, A. Shiran, J. Li, and Y. Liu, "Location independent gesture recognition using channel state information," in *Annual Consumer Communications & Networking Conference*. IEEE, 2022, pp. 841–846.

[165] Y.-J. Chen, W. Chen, S. Q. Zhang, H.-Y. Huang, and H. Kung, "A task-oriented deep learning approach for human localization," *IEEE TCDS*, 2024.

[166] Z. Hao, J. Niu, X.-c. Dang, and Z. Qiao, "Wi-piga: A personnel-independent method for actions recognition based on wi-fi," in *BigCom*. IEEE, 2021, pp. 52–59.

[167] B. Wu, T. Jiang, J. Yu, X. Ding, S. Wu, and Y. Zhong, "Device-free human activity recognition with identity-based transfer mechanism," in *WCNC*. IEEE, 2021, pp. 1–6.

[168] Q. Zhou, Q. Yang, and J. Xing, "Enabling efficient wifi-based occupant behavior recognition using insufficient samples," *Building and Environment*, vol. 212, p. 108806, 2022.

[169] Z. Wei, W. Chen, W. Tao, S. Ning, B. Lian, X. Sun, and J. Zhao, "Catfsid: A few-shot human identification system based on cross-domain adversarial training," *Computer Communications*, vol. 224, pp. 275–284, 2024.

[170] Q. Bu, X. Ming, J. Hu, T. Zhang, J. Feng, and J. Zhang, "Transfersense: towards environment independent and one-shot wifi sensing," *Personal and Ubiquitous Computing*, pp. 1–19, 2022.

[171] Y. Liu, A. Yu, L. Wang, B. Guo, Y. Li, E. Yi, and D. Zhang, "Unifi: A unified framework for generalizable gesture recognition with wi-fi signals using consistency-guided multi-view networks," *IMWUT*, vol. 7, no. 4, pp. 1–29, 2024.

[172] X. Zhang, J. Huang, H. Yan, P. Zhao, G. Zhuang, Z. Liu, and B. Liu, "Wiopen: A robust wi-fi-based open-set gesture recognition framework," *arXiv preprint arXiv:2402.00822*, 2024.

[173] Z. Wu, A. A. Efros, and S. X. Yu, "Improving generalization via scalable neighborhood component analysis," in *ECCV*, 2018, pp. 685–701.

[174] C. Xiao, S. Chen, F. Zhou, and J. Wu, "Self-supervised few-shot time-series segmentation for activity recognition," *IEEE TMC*, vol. 22, no. 11, pp. 6770–6783, 2022.

[175] K. Xu, J. Wang, L. Zhang, H. Zhu, and D. Zheng, "Dual-stream contrastive learning for channel state information based human activity recognition," *JBHI*, vol. 27, no. 1, pp. 329–338, 2022.

[176] Y. Wang, G. Yu, Y. Zhang, D. Liu, and Y. Zhang, "Csi-based location-independent human activity recognition by contrast between dual stream fusion features," *IEEE Sensors Journal*, 2024.

[177] C. Xiao, Y. Han, W. Yang, Y. Hou, F. Shi, and K. Chetty, "Diffusion model-based contrastive learning for human activity recognition," *IoT-J*, 2024.

[178] Y. Liang, H. Li, W. Wu, and P. Xu, "Map-sgan: Multi-anchor point siamese gan for wi-fi csi-based cross-domain gait recognition," *ESWA*, vol. 251, p. 124083, 2024.

[179] Z. Zhao, T. Chen, Z. Cai, X. Li, H. Li, Q. Chen, and G. Zhu, "Crossfi: A cross domain wi-fi sensing framework based on siamese network," *arXiv preprint arXiv:2408.10919*, 2024.

[180] J. Wang, Q. Gao, X. Ma, Y. Zhao, and Y. Fang, "Learning to sense: Deep learning for wireless sensing with less training efforts," *IEEE Wireless Communications*, vol. 27, no. 3, pp. 156–162, 2020.

[181] P. Hu, C. Tang, K. Yin, and X. Zhang, "Wigr: a practical wi-fi-based gesture recognition system with a lightweight few-shot network," *Applied Sciences*, vol. 11, no. 8, p. 3329, 2021.

[182] L. Zhang, S. Wu, T. Zhang, and Q. Zhang, "Learning to locate: Adaptive fingerprint-based localization with few-shot relation learning in dynamic indoor environments," *IEEE TWC*, vol. 22, no. 8, pp. 5253–5264, 2023.

[183] R. Zhang, C. Jiang, S. Wu, Q. Zhou, X. Jing, and J. Mu, "Wi-fi sensing for joint gesture recognition and human identification from few samples in human-computer interaction," *IEEE JASAC*, vol. 40, no. 7, pp. 2193–2205, 2022.

[184] Z. Shi, Q. Cheng, J. A. Zhang, and R. Y. Da Xu, "Environment-robust wifi-based human activity recognition using enhanced csi and deep learning," *IoT-J*, vol. 9, no. 24, pp. 24 643–24 654, 2022.

[185] Z. Shi, J. A. Zhang, R. Xu, Q. Cheng, and A. Pearce, "Towards environment-independent human activity recognition using deep learning and enhanced csi," in *IEEE GLOBECOM*. IEEE, 2020, pp. 1–6.

[186] Z. Shi, J. A. Zhang, R. Y. Xu, and Q. Cheng, "Environment-robust device-free human activity recognition with channel-state-information enhancement and one-shot learning," *IEEE TMC*, vol. 21, no. 2, pp. 540–554, 2020.

[187] T. Zhao, N. Wang, G. Cao, S. Mao, and X. Wang, "Functional data analysis assisted cross-domain wi-fi sensing using few-shot learning," in *IEEE ICC*. IEEE, 2024, pp. 4780–4785.

[188] X. Ding, T. Jiang, Y. Zhong, Y. Huang, and Z. Li, "Wi-fi-based location-independent human activity recognition via meta learning," *Sensors*, vol. 21, no. 8, p. 2654, 2021.

[189] X. Ding, T. Jiang, Y. Zhong, J. Yang, Y. Huang, and Z. Li, "Device-free location-independent human activity recognition via few-shot learning," in *IEEE/CIC ICC in China*, 2021, pp. 106–111.

[190] Y. Gu, H. Yan, M. Dong, M. Wang, X. Zhang, Z. Liu, and F. Ren, "WiOne: one-shot learning for environment-robust device-free user authentication via commodity wi-fi in man-machine system," *IEEE Transactions on Computational Social Systems*, vol. 8, no. 3, pp. 630–642, 2021.

[191] D. Wang, J. Yang, W. Cui, L. Xie, and S. Sun, "Caution: A robust wifi-based human authentication system via few-shot open-set recognition," *IoT-J*, vol. 9, no. 18, pp. 17 323–17 333, 2022.

[192] B. Yang, H. Wang, L. Hu, H. Zhu, C.-T. Lam, and K. Fang, "Few-shot cross-domain based wifi sensing system for online learning in iot," *IEEE Sensors Journal*, 2023.

[193] X. Zhang, C. Tang, K. Yin, and Q. Ni, "Wifi-based cross-domain gesture recognition via modified prototypical networks," *IoT-J*, vol. 9, no. 11, pp. 8584–8596, 2021.

[194] C. Finn, P. Abbeel, and S. Levine, "Model-agnostic meta-learning for fast adaptation of deep networks," in *ICML*. PMLR, 2017, pp. 1126–1135.

[195] S. Huang, Y. Chen, D. Wu, G. Yu, and Y. Zhang, "Few-shot learning for human activity recognition based on csi," in *CACML*. IEEE, 2022, pp. 403–409.

[196] Z. Zhou, F. Wang, J. Yu, J. Ren, Z. Wang, and W. Gong, "Target-oriented semi-supervised domain adaptation for wifi-based har," in *IEEE INFOCOM*. IEEE, 2022, pp. 420–429.

[197] J. Gao, D. Wu, F. Yin, Q. Kong, L. Xu, and S. Cui, "Metaloc: Learning to learn wireless localization," *IEEE JASAC*, 2023.

[198] B. Sheng, R. Han, F. Xiao, Z. Guo, and L. Gui, "Metaformer: Domain-adaptive wifi sensing with only one labelled target sample," *IMWUT*, vol. 8, no. 1, pp. 1–27, 2024.

[199] S. Ding, Z. Chen, T. Zheng, and J. Luo, "Rf-net: A unified meta-learning framework for rf-enabled one-shot human activity recognition," in *SenSys*, 2020, pp. 517–530.

[200] Z. Gao, J. Xue, J. Zhang, and W. Xiao, "MI-wigr: A meta-learning-based approach for cross-domain device-free gesture recognition," *Soft Computing*, vol. 26, no. 13, pp. 6145–6155, 2022.

[201] Y. Zhang, X. Wang, Y. Wang, and H. Chen, "Human activity recognition across scenes and categories based on csi," *IEEE TMC*, 2020.

[202] J. Zhang, Y. Dai, J. Chen, C. Luo, B. Wei, V. C. Leung, and J. Li, "Sida: Self-supervised imbalanced domain adaptation for sound enhancement and cross-domain wifi sensing," *IMWUT*, vol. 7, no. 3, pp. 1–24, 2023.

[203] T. Huang, S. Wang, and S. Li, "Low-cost and user independent action recognition using wifi signals," Available at *SSRN 4160593*.

[204] Y. Wang, L. Yao, Y. Wang, and Y. Zhang, "Robust csi-based human activity recognition with augment few shot learning," *IEEE Sensors Journal*, vol. 21, no. 21, pp. 24 297–24 308, 2021.

[205] L. Zhang, Y. Jiang, Y. Ma, S. Mao, W. Huang, Z. Yu, X. Zheng, L. Shu, X. Fan, and G. Xu, "Toward robust and effective behavior based user authentication with off-the-shelf wi-fi," *IEEE TIFS*, 2024.

[206] C. Xiao, D. Han, Y. Ma, and Z. Qin, "Csigan: Robust channel state information-based activity recognition with gans," *IoT-J*, vol. 6, no. 6, pp. 10 191–10 204, 2019.

[207] X. Chen, H. Li, C. Zhou, X. Liu, D. Wu, and G. Dudek, "Fido: Ubiquitous fine-grained wifi-based localization for unlabelled users via domain adaptation," in *Proceedings of The Web Conference*, 2020, pp. 23–33.

[208] D. Yan, F. Shang, P. Yang, F. Han, Y. Yan, and X.-Y. Li, "freeloc: Wireless-based cross-domain device-free fingerprints localization to free user's motions," *IoT-J*, vol. 11, no. 14, pp. 25 099–25 110, 2024.

[209] B. Zhou, R. Zhou, Y. Luo, and Y. Cheng, "Towards cross domain csi action recognition through one-shot bimodal domain adaptation," in *MobiQuitous*. Springer, 2022, pp. 290–309.

[210] F. Wang, J. Han, S. Zhang, X. He, and D. Huang, "Csi-net: Unified human body characterization and pose recognition," *arXiv preprint arXiv:1810.03064*, 2018.

[211] B. Lan, F. Wang, L. Xia, F. Nai, S. Nie, H. Ding, and J. Han, "Bulldetect: Detecting school physical bullying with wi-fi and deep wavelet transformer," *IoT-J*, 2024.

[212] H. He, X. Huan, J. Wang, Y. Luo, H. Hu, and J. An, "P3id: A privacy-preserving person identification framework towards multi-environments based on transfer learning," *IEEE TMC*, pp. 1–16, 2024.

[213] H. Liu, L. Xi, W. Wang, F. Zhang, and Z. J. Haas, "Openfi: Open-set wifi human sensing via virtual embedding confidence-aware," *IEEE TNSE*, pp. 1–12, 2024.

[214] T. DeVries and G. W. Taylor, "Improved regularization of convolutional neural networks with cutout," *arXiv preprint arXiv:1708.04552*, 2017.

[215] W. Hou and C. Wu, "Rfboost: Understanding and boosting deep wifi sensing via physical data augmentation," *IMWUT*, vol. 8, no. 2, pp. 1–26, 2024.

[216] S. Liu, Z. Chen, M. Wu, H. Wang, B. Xing, and L. Chen, "Generalizing wireless cross-multiple-factor gesture recognition to unseen domains," *IEEE TMC*, 2023.

[217] A. Virmani and M. Shahzad, "Position and orientation agnostic gesture recognition using wifi," in *MobiSys*, 2017, pp. 252–264.

[218] S. Wang, L. Wang, and W. Liu, "Feature decoupling and regeneration towards wifi-based human activity recognition," *Pattern Recognition*, vol. 153, p. 110480, 2024.

[219] B.-B. Zhang, D. Zhang, Y. Li, Y. Hu, and Y. Chen, "Unsupervised domain adaptation for rf-based gesture recognition," *IoT-J*, vol. 10, no. 23, pp. 21 026–21 038, 2023.

[220] Y.-S. Chen, Y.-C. Chang, and C.-Y. Li, "A semi-supervised transfer learning with dynamic associate domain adaptation for human activity recognition using wifi signals," *Sensors*, vol. 21, no. 24, p. 8475, 2021.

[221] J. K. Brinke and N. Meratnia, "Scaling activity recognition using channel state information through convolutional neural networks and transfer learning," in *Proceedings of the International Workshop on Challenges in Artificial Intelligence and Machine Learning for Internet of Things*, 2019, pp. 56–62.

[222] Y. Fang, B. Sheng, H. Wang, and F. Xiao, "Witransfer: A cross-scene transfer activity recognition system using wifi," in *TURC*, 2020, pp. 59–63.

[223] G. Yin, J. Zhang, G. Shen, and Y. Chen, "Fewsense, towards a scalable and cross-domain wi-fi sensing system using few-shot learning," *IEEE TMC*, vol. 23, no. 1, pp. 453–468, 2022.

[224] L. Zheng, S. Bi, S. Wang, Z. Quan, X. Li, X. Lin, and H. Wang, "Resmon: Domain-adaptive wireless respiration state monitoring via few-shot bayesian deep learning," *IoT-J*, vol. 10, no. 23, pp. 20914–20927, 2023.

[225] S. Bi, X. Chen, L. Zheng, H. Hou, and X. Lin, "Roger: Few-shot learning based robust gesture recognition with multi-modal wi-fi csi measurements," in *ICMLCN*. IEEE, 2024, pp. 517–522.

[226] H. Hou, S. Bi, L. Zheng, X. Lin, and Z. Quan, "Sample-efficient cross-domain wifi indoor crowd counting via few-shot learning," in *WOCC*. IEEE, 2022, pp. 132–137.

[227] H. Hou, S. Bi, L. Zheng, X. Lin, Y. Wu, and Z. Quan, "Dasecount: Domain-agnostic sample-efficient wireless indoor crowd counting via few-shot learning," *IoT-J*, vol. 10, no. 8, pp. 7038–7050, 2022.

[228] S. M. Hernandez and E. Bulut, "Wifederated: Scalable wifi sensing using edge-based federated learning," *IoT-J*, vol. 9, no. 14, pp. 12 628–12 640, 2021.

[229] H. Geng, D. Deng, W. Zhang, P. Ji, and X. Wu, "Personalized federated learning based on bidirectional knowledge distillation for wifi gesture recognition," *Electronics*, vol. 12, no. 24, p. 5016, 2023.

[230] X. Li, F. Song, M. Luo, K. Li, L. Chang, X. Chen, and Z. Wang, "Towards collaborative and cross-domain wi-fi sensing: A case study for human activity recognition," *IEEE TMC*, vol. 23, no. 2, pp. 1674–1688, 2023.

[231] W. Qi, R. Zhang, J. Zhou, H. Zhang, Y. Xie, and X. Jing, "A resource-efficient cross-domain sensing method for device-free gesture recognition with federated transfer learning," *IEEE TGCN*, vol. 7, no. 1, pp. 393–400, 2023.

[232] S. Zhang, T. Jiang, X. Ding, Y. Zhong, and H. Jia, "A cloud-edge collaborative framework for cross-environment human action recognition based on wi-fi," in *IEEE/CIC ICC in China*, 2023, pp. 1–6.

[233] N. Zheng, Y. Li, S. Jiang, Y. Li, R. Yao, C. Dong, T. Chen, Y. Yang, Z. Yin, and Y. Liu, "Adawifi, collaborative wifi sensing for cross-environment adaptation," *IEEE TMC*, pp. 1–15, 2024.

[234] J. Zhang, Y. Li, Q. Li, and W. Xiao, "Variance-constrained local-global modeling for device-free localization under uncertainties," *IEEE TH*, 2023.

[235] Y. Bai, Z. Wang, K. Zheng, X. Wang, and J. Wang, "Widrive: Adaptive wifi-based recognition of driver activity for real-time and safe takeover," in *ICDCS*. IEEE, 2019, pp. 901–911.

[236] E. Soltanaghaei, R. A. Sharma, Z. Wang, A. Chittilappilly, A. Luong, E. Giler, K. Hall, S. Elias, and A. Rowe, "Robust and practical wifi human sensing using on-device learning with a domain adaptive model," in *Proceedings of the ACM International Conference on Systems for Energy-Efficient Buildings, Cities, and Transportation*, 2020, pp. 150–159.

[237] S. Zhai, Z. Tang, P. Nurmi, D. Fang, X. Chen, and Z. Wang, "Rise: Robust wireless sensing using probabilistic and statistical assessments," in *MobiCom*, 2021, pp. 309–322.

[238] Q. Fu, F. Wang, M. Zhu, H. Ding, J. Han, and T. X. Han, "Ccs: Continuous learning for customized incremental wireless sensing services," *arXiv preprint arXiv:2412.04821*, 2024.

[239] T. Zhang, Q. Fu, H. Ding, G. Wang, and F. Wang, "Carec: Continual wireless action recognition with expansion-compression coordination," *Sensors*, 2025.

[240] Y. Zhang, F. He, Y. Wang, D. Wu, and G. Yu, "Csi-based cross-scene human activity recognition with incremental learning," *Neural Computing and Applications*, vol. 35, no. 17, pp. 12 415–12 432, 2023.

[241] Y. Ganin, E. Ustinova, H. Ajakan, P. Germain, H. Larochelle, F. Laviolette, M. March, and V. Lempitsky, "Domain-adversarial training of neural networks," *JMLR*, vol. 17, no. 59, pp. 1–35, 2016.

[242] K. Zhou, Z. Liu, Y. Qiao, T. Xiang, and C. C. Loy, "Domain generalization: A survey," *IEEE Transactions on Pattern Analysis and Machine Intelligence*, vol. 45, no. 4, pp. 4396–4415, 2022.

[243] C. Chen, G. Zhou, and Y. Lin, "Cross-domain wifi sensing with channel state information: A survey," *ACM Computing Surveys*, vol. 55, no. 11, pp. 1–37, 2023.

[244] Z. Wang, J. Li, W. Wang, Z. Dong, Q. Zhang, and Y. Guo, "Review of few-shot learning application in csi human sensing," *Artificial Intelligence Review*, vol. 57, no. 8, p. 195, 2024.

[245] X. Wang, K. Niu, J. Xiong, B. Qian, Z. Yao, T. Lou, and D. Zhang, "Placement matters: Understanding the effects of device placement for wifi sensing," *IMWUT*, vol. 6, no. 1, pp. 1–25, 2022.

[246] N. Golyandina, V. Nekrutkin, and A. A. Zhigljavsky, *Analysis of time series structure: SSA and related techniques*. CRC press, 2001.

[247] K. Dragomiretskiy and D. Zosso, "Variational mode decomposition," *IEEE Transactions on Signal Processing*, vol. 62, no. 3, pp. 531–544, 2013.

[248] E. Tzeng, J. Hoffman, K. Saenko, and T. Darrell, "Adversarial discriminative domain adaptation," in *CVPR*, 2017, pp. 7167–7176.

[249] M. Hassan, T. Kelsey, and F. Rahman, "Adversarial ai applied to cross-user inter-domain and intra-domain adaptation in human activity recognition using wireless signals," *Plos one*, vol. 19, no. 4, p. e0298888, 2024.

[250] L. Li, L. Wang, B. Han, X. Lu, Z. Zhou, and B. Lu, "Subdomain adaptive learning network for cross-domain human activities recognition using wifi with csi," in *ICPADS*. IEEE, 2021, pp. 1–7.

[251] R. Remus, "Domain adaptation using domain similarity-and domain complexity-based instance selection for cross-domain sentiment analysis," in *International Conference on Data Mining Workshops*. IEEE, 2012, pp. 717–723.

[252] I. Goodfellow, J. Pouget-Abadie, M. Mirza, B. Xu, D. Warde-Farley, S. Ozair, A. Courville, and Y. Bengio, "Generative adversarial nets," *NeurIPS*, vol. 27, 2014.

[253] J.-Y. Zhu, T. Park, P. Isola, and A. A. Efros, "Unpaired image-to-image translation using cycle-consistent adversarial networks," in *ICCV*, 2017, pp. 2223–2232.

[254] T. Karras, S. Laine, and T. Aila, "A style-based generator architecture for generative adversarial networks," in *CVPR*, 2019, pp. 4401–4410.

[255] J. Devlin, M.-W. Chang, K. Lee, and K. Toutanova, "Bert: Pre-training of deep bidirectional transformers for language understanding," in *NAACL: Human Language Technologies*, 2019, pp. 4171–4186.

[256] O. Ronneberger, P. Fischer, and T. Brox, "U-net: Convolutional networks for biomedical image segmentation," in *MICCAI*. Springer, 2015, pp. 234–241.

[257] A. Jaiswal, R. Y. Wu, W. Abd-Almageed, and P. Natarajan, "Unsupervised adversarial invariance," *NeurIPS*, vol. 31, 2018.

[258] V. Dumoulin, J. Shlens, and M. Kudlur, "A learned representation for artistic style," *arXiv preprint arXiv:1610.07629*, 2016.

[259] M. I. Belghazi, A. Baratin, S. Rajeswar, S. Ozair, Y. Bengio, A. Courville, and R. D. Hjelm, "Mine: mutual information neural estimation," *arXiv preprint arXiv:1801.04062*, 2018.

[260] A. Bulling, U. Blanke, and B. Schiele, "A tutorial on human activity recognition using body-worn inertial sensors," *ACM Computing Surveys*, vol. 46, no. 3, pp. 1–33, 2014.

[261] C. Xiao, Y. Lei, Y. Ma, F. Zhou, and Z. Qin, "Deepseg: Deep-learning-based activity segmentation framework for activity recognition using wifi," *IoT-J*, vol. 8, no. 7, pp. 5669–5681, 2020.

[262] J. Ho, A. Jain, and P. Abbeel, "Denoising diffusion probabilistic models," *NeurIPS*, vol. 33, pp. 6840–6851, 2020.

[263] G. Koch, R. Zemel, and R. Salakhutdinov, "Siamese neural networks for one-shot image recognition," in *ICML Deep Learning Workshop*, vol. 2, no. 1. Lille, 2015, pp. 1–30.

[264] F. Sung, Y. Yang, L. Zhang, T. Xiang, P. H. Torr, and T. M. Hospedales, "Learning to compare: Relation network for few-shot learning," in *CVPR*, 2018, pp. 1199–1208.

[265] O. Vinyals, C. Blundell, T. Lillicrap, and D. Wierstra, "Matching networks for one shot learning," *NeurIPS*, vol. 29, 2016.

[266] X. Ding, T. Jiang, Y. Zhong, S. Wu, J. Yang, and W. Xue, "Improving wifi-based human activity recognition with adaptive initial state via one-shot learning," in *WCNC*. IEEE, 2021, pp. 1–6.

[267] A. Nichol, "On first-order meta-learning algorithms," *arXiv preprint arXiv:1803.02999*, 2018.

[268] J. Oh, H. Yoo, C. Kim, and S.-Y. Yun, "Boil: Towards representation change for few-shot learning," *arXiv preprint arXiv:2008.08882*, 2020.

[269] M. Andrychowicz, M. Denil, S. Gomez, M. W. Hoffman, D. Pfau, T. Schaul, B. Shillingford, and N. De Freitas, "Learning to learn by gradient descent by gradient descent," *NeurIPS*, vol. 29, 2016.

[270] I. Gulrajani, F. Ahmed, M. Arjovsky, V. Dumoulin, and A. C. Courville, "Improved training of wasserstein gans," *NeurIPS*, vol. 30, 2017.

[271] A. Makhzani, J. Shlens, N. Jaitly, I. Goodfellow, and B. Frey, "Adversarial autoencoders," *arXiv preprint arXiv:1511.05644*, 2015.

[272] S. Shalev-Shwartz, "Online learning and online convex optimization," *Foundations and Trends® in Machine Learning*, vol. 4, no. 2, pp. 107–194, 2012.

[273] A. P. Dempster, N. M. Laird, and D. B. Rubin, "Maximum likelihood from incomplete data via the em algorithm," *Journal of the Royal Statistical Society: Series B (Methodological)*, vol. 39, no. 1, pp. 1–22, 1977.

[274] B. Zhao, X. Xiao, G. Gan, B. Zhang, and S.-T. Xia, "Maintaining discrimination and fairness in class incremental learning," in *CVPR*, 2020, pp. 13 208–13 217.

[275] J. Kirkpatrick, R. Pascanu, N. Rabinowitz, J. Veness, G. Desjardins, A. A. Rusu, K. Milan, J. Quan, T. Ramalho, A. Grabska-Barwinska, D. Hassabis, C. Clopath, D. Kumaran, and R. Hadsell, "Overcoming catastrophic forgetting in neural networks," *Proceedings of the National Academy of Sciences*, vol. 114, no. 13, pp. 3521–3526, 2017.

[276] D. Halperin, W. Hu, A. Sheth, and D. Wetherall, "Tool release: Gathering 802.11 n traces with channel state information," *ACM SIGCOMM Computer Communication Review*, vol. 41, no. 1, pp. 53–53, 2011.

[277] E. Yi, D. Wu, J. Xiong, F. Zhang, K. Niu, W. Li, and D. Zhang, " $\{\text{BFMSense}\}:\{\text{WiFi}\}$ sensing using beamforming feedback matrix," in *NSDI*, 2024, pp. 1697–1712.

[278] F. Gringoli, M. Schulz, J. Link, and M. Hollick, "Free your csi: A channel state information extraction platform for modern wi-fi chipsets," in *WiNTECH*, 2019, pp. 21–28.

[279] M. Atif, S. Muralidharan, H. Ko, and B. Yoo, "Wi-esp—a tool for csi-based device-free wi-fi sensing (dfws)," *Journal of Computational Design and Engineering*, vol. 7, no. 5, pp. 644–656, 2020.

[280] Z. Wang, F. Li, H. Zhao, Z. Mao, Y. Zhang, Q. Huang, B. Cao, M. Cao, B. He, and Q. Hou, "Wi-fi sensing tool release: Gathering 802.11 ax channel state information from a commercial wi-fi access point," *arXiv preprint arXiv:2506.16957*, 2025.

[281] Z. Jiang, T. H. Luan, X. Ren, D. Lv, H. Hao, J. Wang, K. Zhao, W. Xi, Y. Xu, and R. Li, "Eliminating the barriers: Demystifying wi-fi baseband design and introducing the picoscenes wi-fi sensing platform," *IoT-J*, vol. 9, no. 6, pp. 4476–4496, 2021.

[282] R. Li, Y. Duan, R. Du, F. Xu, H. Zhao, Y. Sun, Y. Zhang, D. Zhang, Y. Liu, Z. Jiang *et al.*, "Reshaping wifi isac with high-coherence hardware capabilities," *IEEE Communications Magazine*, vol. 62, no. 9, pp. 114–120, 2024.

[283] S. Huang, K. Li, D. You, Y. Chen, A. Lin, S. Liu, X. Li, and J. A. McCann, "Wimans: A benchmark dataset for wifi-based multi-user activity sensing," in *ECCV*. Springer, 2024, pp. 72–91.

[284] Z. Zhao, T. Chen, F. Meng, H. Li, X. Li, and G. Zhu, "Finding the missing data: A bert-inspired approach against package loss in wireless sensing," *arXiv preprint arXiv:2403.12400*, 2024.

[285] C. Zhang and W. Jiao, "Imgfi: A high accuracy and lightweight human activity recognition framework using csi image," *IEEE Sensors Journal*, 2023.

[286] F. Meneghelli, N. Dal Fabbro, D. Garlisi, I. Tinnirello, and M. Rossi, "A csi dataset for wireless human sensing on 80 mhz wi-fi channels," *IEEE Communications Magazine*, vol. 61, no. 9, pp. 146–152, 2023.

[287] F. Demrozi, C. Turetta, A. Masrur, M. Schmidhammer, C. Gentner, S. Chakraborty, G. Pravadelli, and P. Kindt, "A dataset on csi-based activity recognition in real-world environments," *Authorea Preprints*, 2023.

[288] J. Yang, X. Chen, H. Zou, D. Wang, Q. Xu, and L. Xie, "Efficientfi: Toward large-scale lightweight wifi sensing via csi compression," *IoT-J*, vol. 9, no. 15, pp. 13 086–13 095, 2022.

[289] Z. Yang, Y. Zhang, and Q. Zhang, "Rethinking fall detection with wifi," *IEEE TMC*, vol. 22, no. 10, pp. 6126–6143, 2022.

[290] M. J. Bocus, W. Li, S. Vishwakarma, R. Kou, C. Tang, K. Woodbridge, I. Craddock, R. McConvile, R. Santos-Rodriguez, K. Chetty, and R. Piechocki, "Operanet: a multimodal activity recognition dataset acquired from radio frequency and vision-based sensors," *Scientific data*, vol. 9, no. 1, p. 474, 2022.

[291] P. F. Moshiri, R. Shahbazian, M. Nabati, and S. A. Ghorashi, "A csi-based human activity recognition using deep learning," *Sensors*, vol. 21, no. 21, p. 7225, 2021.

[292] R. Alazrai, A. Awad, A. Bahaa'A, M. Hababeh, and M. I. Daoud, "A dataset for wi-fi-based human-to-human interaction recognition," *Data in brief*, vol. 31, p. 105668, 2020.

[293] A. Bahaa'A, M. M. Almazari, R. Alazrai, and M. I. Daoud, "A dataset for wi-fi-based human activity recognition in line-of-sight and non-line-of-sight indoor environments," *Data in Brief*, vol. 33, p. 106534, 2020.

[294] L. Guo, L. Wang, C. Lin, J. Liu, B. Lu, J. Fang, Z. Liu, Z. Shan, J. Yang, and S. Guo, "Wiar: A public dataset for wifi-based activity recognition," *IEEE Access*, vol. 7, pp. 154 935–154 945, 2019.

[295] J. K. Brinke and N. Meratnia, "Dataset: Channel state information for different activities, participants and days," in *Proceedings of Workshop on Data Acquisition to Analysis*, 2019, pp. 61–64.

[296] B. Lan, P. Li, J. Yin, Y. Song, G. Wang, H. Ding, J. Han, and F. Wang, "Xrf v2: A dataset for action summarization with wi-fi signals, and imus in phones, watches, earbuds, and glasses," *arXiv preprint arXiv:2501.19034*, 2025.

[297] B.-J. Chen and R. Y. Chang, "Few-shot transfer learning for device-free fingerprinting indoor localization," in *ICC*. IEEE, 2022, pp. 4631–4636.

[298] T. X. Han, R. Du, Z. Tang, and Y. Cui, "Public dataset of the first wi-fi sensing contest," 2024, <http://www.sdp8.org/Dataset?id=277beeba-afdc-4bb1-8b47-88fa366fb27d>, <http://www.sdp8.org/Dataset?id=787a9a88-d2f3-4944-a174-8edf6070c99a>.

[299] Z. Liu, L. Zhang, B. Li, Y. Zhou, Z. Chen, and C. Zhu, "Wifi csi based temporal activity detection via dual pyramid network," in *AAAI*, vol. 39, no. 1, 2025, pp. 550–558.

[300] A. Krizhevsky, I. Sutskever, and G. E. Hinton, "Imagenet classification with deep convolutional neural networks," in *NeurIPS*, vol. 25, 2012, pp. 1097–1105.

[301] J. Deng, W. Dong, R. Socher, L.-J. Li, K. Li, and L. Fei-Fei, "Imagenet: A large-scale hierarchical image database," in *CVPR*. IEEE, 2009, pp. 248–255.

[302] T.-Y. Lin, M. Maire, S. Belongie, J. Hays, P. Perona, D. Ramanan, P. Dollár, and C. L. Zitnick, "Microsoft coco: Common objects in context," in *ECCV*. Springer, 2014, pp. 740–755.

[303] W. Kay, J. Carreira, K. Simonyan, B. Zhang, C. Hillier, S. Vijayanarasimhan, F. Viola, T. Green, T. Back, P. Natsev, M. Suleyman, and A. Zisserman, "The kinetics human action video dataset," *arXiv preprint arXiv:1705.06950*, 2017.

[304] D. P. Kingma and M. Welling, "Auto-encoding variational bayes," *arXiv preprint arXiv:1312.6114*, 2013.

[305] B. Mildenhall, P. P. Srinivasan, M. Tancik, J. T. Barron, R. Ramamoorthi, and R. Ng, "Nerf: Representing scenes as neural radiance fields for view synthesis," *Communications of the ACM*, vol. 65, no. 1, pp. 99–106, 2021.

[306] B. Kerbl, G. Kopanas, T. Leimkühler, and G. Drettakis, "3d gaussian splatting for real-time radiance field rendering," *ACM ToG*, vol. 42, no. 4, pp. 139–1, 2023.

[307] A. Raistrick, L. Mei, K. Kayan, D. Yan, Y. Zuo, B. Han, H. Wen, M. Parikh, S. Alexopoulos, L. Lipson, Z. Ma, and J. Deng, "Infinigen indoors: Photorealistic indoor scenes using procedural generation," in *CVPR*, 2024, pp. 21 783–21 794.

[308] M. M. Loper, N. Mahmood, J. Romero, G. Pons-Moll, and M. J. Black, "Smpl: A skinned multi-person linear model," *ACM ToG*, vol. 34, no. 6, pp. 1–16, 2015.

[309] J. Romero, D. Tzionas, and M. J. Black, "Embodied hands: Modeling and capturing hands and bodies together," *arXiv preprint arXiv:2201.02610*, 2022.

[310] A. Radford, J. W. Kim, C. Hallacy, A. Ramesh, G. Goh, S. Agarwal, G. Sastry, A. Askell, P. Mishkin, J. Clark, G. Krueger, and I. Sutskever, "Learning transferable visual models from natural language supervision," in *ICML*, 2021.

[311] T. B. Brown, B. Mann, N. Ryder, M. Subbiah, J. Kaplan, P. Dhariwal, A. Neelakantan, P. Shyam, G. Sastry, A. Askell, S. Agarwal, A. Herbert-Voss, G. Krueger, T. Henighan, R. Child, A. Ramesh, D. M. Ziegler, J. Wu, C. Winter, C. Hesse, M. Chen, E. Sigler, M. Litwin, S. Gray, B. Chess, J. Clark, C. Berner, S. McCandlish, A. Radford, I. Sutskever, and D. Amodei, "Language models are few-shot learners," *NeurIPS*, vol. 33, pp. 1877–1901, 2020.

[312] A. Vaswani, N. Shazeer, N. Parmar, J. Uszkoreit, L. Jones, A. Gomez, L. Kaiser, and I. Polosukhin, "Attention is all you need," in *NeurIPS*, 2017.

[313] A. Gu and T. Dao, "Mamba: Linear-time sequence modeling with selective state spaces," *arXiv preprint arXiv:2312.00752*, 2023.

[314] K. He, X. Chen, S. Xie, Y. Li, P. Dollár, and R. Girshick, "Masked autoencoders are scalable vision learners," in *CVPR*, 2022, pp. 16 000–16 009.

[315] E. J. Hu, Y. Shen, H. M. Wallach, A. Tsai, and A. M. Dai, "Lora: Low-rank adaptation of large language models," in *ICML*, 2022, pp. 10 163–10 173.

[316] S. A. Rebuffi, H. Bilen, and A. Vedaldi, "Learning multiple visual domains with residual adapters," in *CVPR*, 2017, pp. 506–514.

[317] P. Liu, X. Qiu, and X. Huang, "Pre-train, prompt, and predict: A systematic survey of prompting methods in natural language processing," in *ACL*, 2021, pp. 1–12.

[318] M. Lewis, N. Perez, A. Piktus, F. Petroni, M. Bartl, Y. Wang, H. Schütze, L. Zettlemoyer, and S. Ruder, "Retrieval-augmented generation for knowledge-intensive nlp tasks," in *ICML*, 2020, pp. 10 056–10 068.

[319] S. Han, H. Mao, and W. J. Dally, "Learning both weights and connections for efficient neural networks," in *NeurIPS*, vol. 28, 2015.

[320] B. Jacob, S. Kligys, B. Chen, M. Zhu, P. T. Tang, A. Anand, C.-F. Weng, S. Jäkel, M. McCool, and K. Keutzer, "Quantizing deep convolutional networks for efficient inference: A whitepaper," in *CVPR*, 2018, pp. 2704–2713.

[321] G. Hinton, O. Vinyals, and J. Dean, "Distilling the knowledge in a neural network," in *NeurIPS*, vol. 28, 2015.

[322] W. Shi, J. Cao, Q. Zhang, Y. Li, and L. Xu, "Edge computing: Vision and challenges," *IoT-J*, vol. 3, no. 5, pp. 637–646, 2016.